Research article

Sediment microbial communities of a technogenic saline-alkaline reservoir

Pavel Belkin [a],[*], Yulia Nechaeva [b], Sergey Blinov [a], Sergey Vaganov [a], Roman Perevoshchikov [a], Elena Plotnikova [b]

[a] Natural Science Institute, Perm State University, 614068, Bukireva st. 15, Perm, Russia
[b] Institute of Ecology and Genetics of Microorganisms, Ural Branch of the Russian Academy of Sciences, 614081, Goleva st. 13, Perm, Russia

ARTICLE INFO

ABSTRACT

Various natural saline and alkaline habitats have recently been widely investigated, but knowledge of anthropogenic habitats with more complex environmental conditions is still lacking. This research looks at the structure of microbial communities in 18 bottom sediment samples from a technogenic water body with saline and alkaline composition. The core samples were collected from 2 columns in the western and eastern parts of an artificial water body at the Verkhnekamskoe Salt Deposit (Russia). The microbial community structure was studied using high-throughput 16S rRNA gene sequencing. The bottom sediment composition (salinity, pH, and toxic element content) varies greatly with depth and laterally throughout the study area. The study found a considerable difference in bacterial community diversity between the 2 columns, but no considerable difference was found between the communities at various depths of the studied layers. *Proteobacteria*, *Firmicutes*, and *Actinobacteria*, which are common in both natural and artificial saline and alkaline environments, make up the majority of the bacteria found in the samples. Studies have shown that salinity and total alkalinity are the key factors influencing the formation of microbial communities. *Ralstonia* and *Pseudomonas* were the two most common genera in the sediment samples. These two genera are known for having high metabolic flexibility, which means they can survive in extreme environments and use a variety of carbon compounds as energy sources. The study also found that *Ralstonia* is indicator bacteria in samples with the highest concentrations of toxic elements compared to the other samples. A relatively high microbial diversity was discovered in the studied anthropogenic water reservoir despite the extreme alkaline and saline conditions, but it is considerably lower than that found in natural, less alkaline habitats. This research offers insight into the mechanisms behind microbial community formation in complex anthropogenic environments and covers key factors in microbial community distribution.

1. Introduction

Researchers have recently become more interested in investigating the microorganisms of extreme habitats (extremophiles) with high salinity and alkalinity [1]. Such interest stems from their biological uniqueness, namely their ability to survive and produce

enzymes in harsh environments with high salinity and pH [2]. The possibility of using halophilic and alkalophilic microorganisms for various biotechnological applications (environmental bioremediation, food industry, pharmaceuticals, etc.) is being widely researched [3,4].

Haloalkalophiles, which require both high salinity (up to 33 % NaCl) and alkaline pH (>pH 9), are common in both natural and artificial habitats [5,6]. They are found in extremely saline and alkaline natural environments, such as soda ash lakes and salt lakes [7, 8], salt deposits [9], saline soils [10,11], and salt mines [12,13]. Microbial diversity in the listed natural habitats was found to be highly dependent on temperature, pH, as well as the quantitative and qualitative composition of soluble salts [14,15]. Salinity and high pH of the environment are among the most important factors shaping the prokaryotic community [16,17]. Previous studies have shown that haloalkalophilic bacteria such as *Proteobacteria*, *Firmicutes*, *Bacteroidetes*, *Actinobacteria, Cyanobacteria,* and *Euryarchaeota* predominate in such systems.

However, little is known about the microbial diversity in artificial habitats, such as reservoirs filled with mining wastes, by-products of soda ash and salt production, and water bodies under heavy anthropogenic influence. Similar research have been conducted in Poland [18], Mexico [19], India [20], France [21], the United States [22], and China [23].

The variety of factors affecting waste composition makes investigating technogenic objects challenging. These factors are determined by the specifics of the technological processes and the raw materials used. Industrial waste can be highly saline or have high pH, as well as contain large amounts of toxic impurities or organic pollutants.

Mining waste generated and stored on the territory of the Verkhnekamskoe Salt Deposit (Perm Krai, Russia) is extremely high in water-soluble salts, primarily sodium and potassium chlorides [24–27]. In the Verkhnekamsky industrial district, soda ash production is an important process that takes place in addition to the mining and processing of potassium salts. Since 1883, the Verkhnekamskoe Deposit brine and carbonate rocks have been processed using the Solvay method to produce soda ash.

The Solvay process generates a large amount of waste. This waste is alkaline (pH 10–12), and it contains large amounts of chloride ions, calcium ions, and sodium ions (total dissolved salts can exceed 100 g/L). At the same time, impurities such as toxic metals and arsenic can accumulate in the solid waste. The combination of high salinity and an alkaline environment, which is unique to surface conditions, creates extreme living conditions for microorganisms, the inhabitants of soda ash sludge reservoirs.

The study of the microbial community composition of artificial alkaline sites and the comparison of such systems with natural ecosystems provide new opportunities for the analysis of factors influencing the microbial community structure. Additionally, the lack of knowledge about these sites opens the possibility of discovering and describing new extremophilic microorganisms and evolutionary relationships, which further contributes to a better understanding of global microbial diversity. It is possible to study the processes involved in the formation of extremophilic microbial communities because of the low initial microbial diversity of newly established artificial habitats. This advances the understanding of evolution and establishes the role of environmental factors in the development of microbial communities in naturally formed extreme environments.

Reliable knowledge of halophilic and alkalophilic microorganisms in industrial waste also has practical value. Currently, there is an urgent need in many mining areas to eliminate surface waste storage facilities, which take up many tens or hundreds of hectares and have an intense environmental impact [28]. The mechanical removal and transfer of waste to designated landfills are either expensive or impossible due to the enormous volumes. The potential for on-site industrial waste reclamation, including the use of biotechnological methods, must therefore be taken into account.

Given the foregoing, the goal of this research is to describe the microbial community structure in bottom sediments of a technogenic saline-alkaline water body and to identify the environmental factors that have the biggest impact on the microbial community structure under extreme saline-alkaline conditions.

It is assumed that the conditions created in the alkaline reservoir as a result of the operations in the Verkhnekamsky industrial hub will greatly affect the diversity and structure of microbial communities. When compared to natural saline and alkaline ecosystems, the harsh conditions in this reservoir are expected to lead to a microbial diversity loss. Changes in the composition of microbial communities in columns A and B are also anticipated due to different wastewater influx routes into these sections of the water basin. It is also important to assess the impact of individual sediment layers, particularly those with the highest concentrations of toxic elements, on the microbial community. Furthermore, it is necessary to determine which environmental factors will be essential in the establishment of the microbial community.

2. Materials and methods

2.1. Study area

The object of the research is a technogenic pond that was created in 1960–1970. The pond is located on the former territory of the soda ash plant in Berezniki (Perm Krai, Russia). The pond served as temporary backup storage for the soda ash production waste during the construction of the main sludge reservoir. Following the construction of the main storage facility, the study area continued to be used as a backup reservoir. The pond received wastewater from both the western and eastern sides, as well as from a nearby industrial waste diversion channel that collected wastewater from multiple plants in the Berezniki industrial area. Today, this body of water is located in an urban area and poses a hazard.

The pond currently has a nearly uniform pentagonal shape and is surrounded by dams (Fig. 1). The reservoir has a diameter of 500 m and covers a surface area of 17 ha. The water depth varies throughout the year, but it rarely surpasses 1 m. The primary sources of water supply throughout its existence were atmospheric precipitation and wastewater discharge. The inflow of wastewater into the reservoir has now been completely halted. There is no visible hydraulic connection to other bodies of water. The shoreline of the Kama

River (Kama Reservoir), stretching 150 m to the west, serves as an important water supply source in the area.

During its relatively short existence (approximately 60 years), the reservoir experienced the formation of a thick layer of sediments, which reached a thickness of 4.5 m in certain areas. This rapid sedimentation can be attributed to the substantial deposition of fine calcium carbonate from industrial wastewater. In addition to the soda ash distillate, the pond also received waste from other nearby industries. These included water from fuel oil tank washing, acidic wastewater from titanium and magnesium production, wastewater from organic synthesis facilities, waste from the production of chlorobenzene, lead silicate, sodium metal, caustic mercury, caustic potash, and many others.

Separate layers of a specific composition are formed in the bottom sediments due to the reservoir being filled with industrial wastewater of various compositions, the substances being "preserved" in a strongly alkaline environment, and the lack of a leaching regime due to the dam fencing. This reflects the past industrial activity in the nearby enterprises of the Berezniki industrial area. The possibility of creating special conditions for the growth and development of microbial communities depends on the diversity of the properties and composition of the sediment layers.

2.2. Drilling and sampling methods

In September 2021, bottom sediment samples were collected using sinking columns (wells) and continuous core sampling. Bottom sediments were taken from two locations: A and B (Fig. 1). The coordinates of the sampling sites are: 59°25'15.22 "N, 56°43'59.63 "B (Site A), 59°25'20.36 "N, 56°44'17.38 "B (Site B). The location of wells A and B follows the historical flow paths of the wastewater into the pond on the west and east sides.

The wells were drilled from a floating catamaran platform (Fig. S1). Undisturbed sediments were sampled using a special sampling device [29] and plastic pipes with a diameter of 110 mm. Three wells were drilled on each site, forming an equilateral triangle with sides no longer than 3 m. Sediments from the three wells at each site were examined and described. Identical layers were identified based on the sediment structure, their physical characteristics (colour, density, and moisture), and their organoleptic properties (smell). In total, nine distinct layers of sludge were identified. Combined samples from the two wells were collected from selected layers. This resulted in a total of 18 bottom sediment samples that were collected for further research.
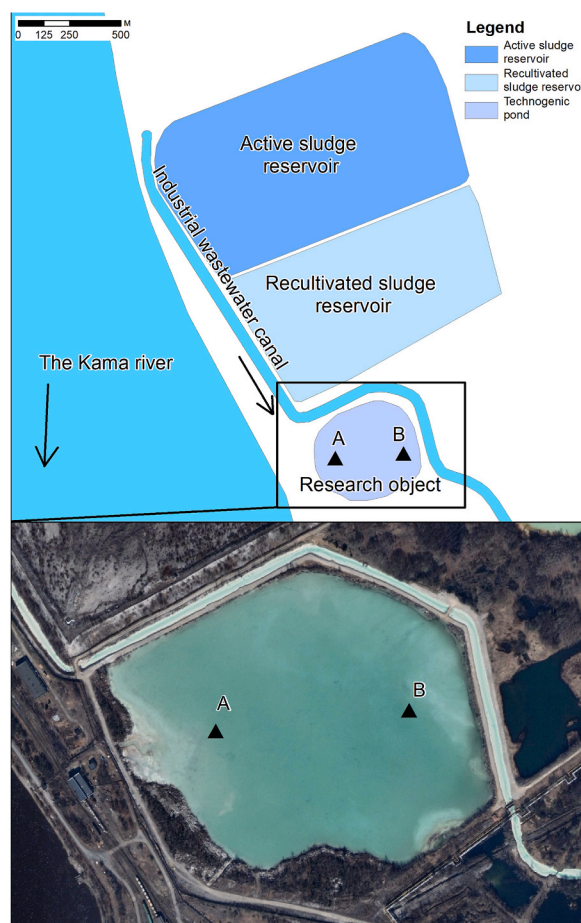

Fig. 1. Study area (A and B - bottom sediment drilling sites).

The samples were carefully placed in sterile containers and stored in a refrigerated container at $+4\,°C$ in order to deliver them to the laboratory. Upon arrival, each sample was divided into two separate parts. One part, which was intended for microbial community research, was stored at $-80\,°C$. The other part was air-dried and then stored at $4\,°C$, which allowed for the analysis of the physico-chemical properties and presence of toxic metals in the samples.

2.3. Methods for studying the physical and chemical properties of sediments

The sieve method was employed to perform granulometric analysis using a 50 g sample. The selected sample was desiccated at $105\,°C$ until it reached a consistent weight. The dried material was divided among lithological sieves with the following cell sizes, in mm: 1, 0.5, 0.25, 0.1, and 0.05. The granulometric composition was then determined.

The hydrogen index was calculated in a lab setting using the potentiometric method (pH-meter Expert, Econix-Expert, Russia). A sample of natural humidity sludge was used to derive a water extract for this purpose in a 1:1 ratio (natural humidity sample to distilled water). The samples were air-dried, and the water extract was prepared in a 1:5 ratio (dry sample to distilled water) to determine the dry residue and alkalinity, as well as cation and anion content. Capillary electrophoresis ("KAPEL-105 M", Econix-Expert, Russia) was used to determine the cations and anions. The total alkalinity was determined through potentiometric titration. The gravimetric method was used to calculate the total amount of dissolved salts (dry residue). After evaporating the water extract samples at $105°C$, the mineral portion was dried and weighed. The ALPHA device (Bruker Optik GmbH, Germany) was used in infrared spectrometry to examine the samples and determine the mass fraction of petroleum products. Calcination to constant mass was used to calculate the total fraction of organic matter, including humus, plant residues, and dispersed organic matter.

Using an Aurora M90 ICP-MS spectrometer (Bruker, Fremont, CA, USA), the amount of toxic trace elements (Zn, Cu, Pb, Ni, Cr, Cd, As, and Hg) in the samples was determined. To prepare the sample, a solution was made through autoclave digestion. Concentrated HNO_3 was used for dissolution. Analysis was conducted using samples weighing 0.1 g. Control (blank) samples and one standard sample were placed together with the analysed samples. To ensure the accuracy of sample analysis, standard samples from the Institute of Geochemistry, Siberian Branch of the Russian Academy of Sciences (Irkutsk, Russia) were used. The validity of the analytical methods was verified by analysing the standard reference material Gabbro Essexit STD-2A (GSO 8670-2005).

2.4. DNA extraction, sequencing, and sequence analysis

Following the manufacturer's instructions, a set of reagents NucleoSpin Soil (MACHEREY-NAGEL, Germany) was used to extract community genomic DNA from a 0.25 g sediment. PCR was used to amplify the hyper variable V4 region of the 16S rRNA gene using the primer pairs 515F/806R (5′-GTGCCAGCMGCCGCGGTAA-3'/5′-GGACTACVSGGGTATCTAAT-3′) [30]. Illumina (USA) was used to modify the primer pairs for each sample to include adapters and unique barcodes. Each sample was subjected to PCR using a 15 μL reaction mixture that included a 0.5–1 activity unit of Q5® High-Fidelity DNA Polymerase (NEB, USA), 5 pcM of forward and reverse primers, 10 ng of a DNA matrix, and 2 nM of each dNTP (LifeTechnologies, USA). The temperature cycling process involved pre-denaturation at $94\,°C$ for 1 min, followed by 25 cycles at $94\,°C$ for 10 s, at $55\,°C$ for 30 s, at $72\,°C$ for 60 s, and a final extension at $72\,°C$ for 3 min. The PCR products were purified using AMPure XP magnetic beads (Beckman Coulter, USA). To profile the prokaryotic community, 16S rRNA amplicon sequencing libraries were prepared according to the manufacturer's instructions (Illumina, USA). The DNA library was sequenced on the Illumina MiSeq platform using a MiSeq® ReagentKit v3 (2×300 bp, 600 cycles).

Illumina software was used to demultiplex 300 bp paired-end reads by MiSeq. FASTQC v0.11.7 [31] was used to verify that the sequencing data quality for all samples meets the required analytical standards. Trimmomatic v0.36 [32] was used to perform pruning of low-quality sequences to ensure the reliability of subsequent analysis. Then sequence quality control, paired-end sequence integration, chimera removal, and identification of ASVs were performed by DADA2 [33] integrated in QIIME 2 version 2021.11 [34] with default parameters. The generated representative sequences were used for taxonomic classification using the naive Bayes classifier, which determines the probability that a sequence belongs to a certain species [35]. The naive Bayes classifier used in this study was pretrained based on SILVA v138 [36]. The q2-feature-classifier script [37] was used to assign taxonomy to ASVs. Taxonomic distributions of the samples were estimated using the q2-taxa-barplot script. Sequences of mitochondria and chloroplasts were filtered out prior to performing diversity analyses.

2.5. Microbial community diversity analysis and statistical analyses

The obtained dataset was used to determine richness (Chao1 estimator), community diversity (Shannon index and Simpson index), and evenness (Pielou's evenness) through QIIME 2 version 2021.11 [34]. The Kruskal-Wallis (pairwise) test was used to analyse group differences in an alpha diversity measure. Beta diversity metrics (Bray-Curtis dissimilarity) were estimated using the q2-diversity plugin (QIIME 2 version 2021.11) after samples were rarefied to 8.339 sequences per sample. This value was used in order to ensure the inclusion of all samples and the greatest number of sequences in the study. The permutational multivariate analysis of variance (PERMANOVA) in QIIME 2 with 9999 permutations was used to analyse differences in beta diversity. The statistical significance was set at $p < 0.05$.

The FactoMineR and phyloseq packages in R were used to perform principal component analysis (PCA) and principal coordinates analysis (PCoA) [38,39]. Redundancy analysis (RDA) was conducted to assess the connection between community composition and environmental parameters using the RDA function of the vegan package for R [40]. Chemical analysis data underwent statistical processing through the implementation of Mann-Whitney and Kolmogorov-Smirnov tests, as well as hierarchical clustering, using the

Statistica 12 software package (StatSoft Inc., Tulsa, USA).

Prior to RDA, variance inflation factor (VIF) was calculated for each environmental variable to measure collinearity. The variable with the highest VIF was discarded until the VIF values for all variables dropped below 10. In RDA, environmental factors were used as explanatory variables to elucidate the variation in microbial communities and were visually represented as arrows, with the microbial communities serving as the objects. The Hmisc package in R was used to calculate and visualise Spearman's correlation coefficients between the physicochemical parameters of the sediment samples and the abundance of phylum [41]. The ggcor package was employed to perform a Mantel test between ASV and environmental parameters. Figures were made using the ggplot2 package [42]. The linear discriminant analysis effect size (LEfSe) algorithm was used to identify distinguishing features that were significant both statistically and biologically (biomarker discovery). A logarithmic LDA (linear discriminant analysis) score >3.5 was set as the threshold to estimate the effect size. Given the complexity of metagenomic profiles, the LEfSe findings were replicated using the analysis of the composition of microbiomes (ANCOM-BC) [43].

3. Results

3.1. Field description of columns and selection of layers

Column A was drilled in the western part of the technogenic pond (Fig. 1). The water depth at the sampling site was 0.40 m. The sediment thickness in the column was 2.13 m. The compaction of bottom sediments during the sampling process did not exceed 10 %. The sediments in the interval from 0 to 0.68 m were mostly dense grey paste, and the interlayers in the interval from 0.51 to 0.68 m were yellow and solid. Bottom sediments in the 0.68–1.04 m interval were dense black paste with red-brown interlayers. In the lower intervals, the sediments appeared as a dense grey paste. A strong chemical odour was present throughout the sampling interval. Based on morphological, visual, and organoleptic characteristics, a total of 9 layers were identified, with thicknesses ranging from 0.09 to 0.57 m (Fig. 2).

Column B was drilled in the eastern part of the pond (Fig. 1). The water depth to the sediment surface was 0.30 m. The sediment thickness in the column was 1.82 m. There was also 10 % compaction of the bottom sediment at the time of sampling. The upper layer (from 0 to 0.12 m) appeared as a homogeneous white paste. The sediments from 0.12 to 0.25 m had a lumpy brown paste-like consistency. In the interval from 0.25 to 0.38 m, the paste was white with black interlayers. The sediment between 0.38 and 0.85 m was a brown paste with red interlayers and inclusions. In the interval from 0.85 to 1.02 m, the sediment was a homogeneous grey-green paste. The lower interval (1.02–1.82 m) consisted of a homogeneous grey and dark grey paste with solid pink particles in the lower
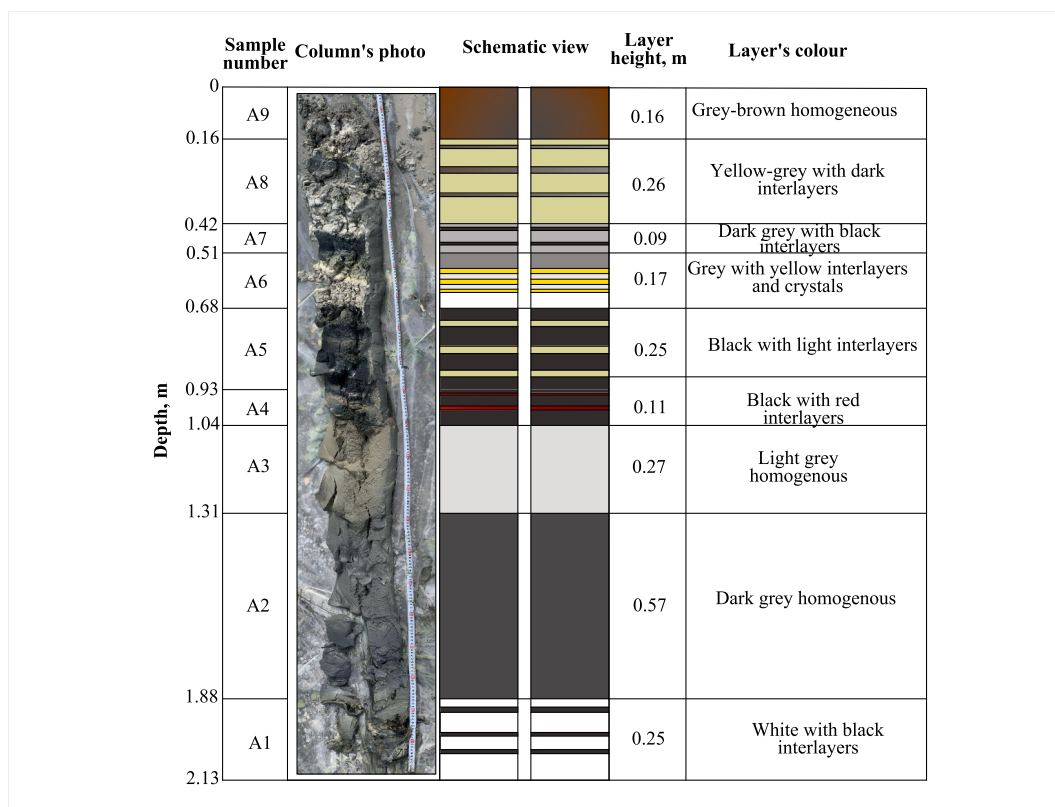

Fig. 2. Sediment section along the column A.

section. The bottom layers of the column had a faint chemical odour. Based on morphological, visual, and organoleptic characteristics, a total of 9 layers were identified, ranging in thickness from 0.12 to 0.31 m (Fig. 3).

A comparison of the visual and organoleptic characteristics of columns A and B revealed similarities in the accumulated sediments at the bottom part of the columns (grey paste of different shades, mostly homogeneous). In addition, thin bright red interlayers were detected in the middle part of the sediment. The upper part of the sludge in columns A and B exhibited visual differences, suggesting a potential variation in the composition of the wastewater that generated the sludge in the previous period.

3.2. Particle size analysis

Particle size analysis was conducted in order to determine the input pathways of bottom sediment constituents. Sedimentation of wastewater was assumed to produce the smallest particles (less than 0.05 mm). Larger particles (dust and sand) were brought in from outside through atmospheric transport. Based on the results obtained from sieving, it was evident that the dominant particle category in both columns was composed of fine particles (less than 0.05 mm).

Coarse particles larger than 1 mm (10–20 %) were present in the upper sediment layers in column A (from A9 to A6), indicating that external particles likely entered the pond sediments through atmospheric transportation. The portion of coarse particles in the lower layers did not exceed 4 %. Within the depth range of 0.5–0.7 m, there were solid interlayers consisting of yellow crystals, measuring approximately 1 cm in thickness, along with some larger yellow crystals.

The sludge in column B displayed a particle size distribution that was more uniform. In nearly all layers, over 90 % of the particles had a size smaller than 0.05 mm. The prevalence of finely dispersed particles shows that sludge is primarily formed through chemical processes when particles settle in a solution. In this area of the reservoir, the amount of extraneous particles entrained in the sludge was considerably lower than in the western part of the area in column A. Table S1 shows the size distribution of sediment particles after undergoing the sieving process.

3.3. Physico-chemical analysis of water extract and the content of toxic trace elements

Table 1 shows the composition of the water extracts derived from the sludge layers in the columns. The water extract from the A-column sludge was strongly alkaline, with pH values ranging from 11.2 to 11.6 depending on the thickness of the sediment. The layers A6–A8 exhibited the highest total alkalinity, ranging from 33 to 41 mg-eq/L, while the remaining layers showed alkalinity levels between 7 and 16 mg-eq/L. Similarly, the water extract derived from the B-column sludge exhibited a strong alkaline nature, but with a
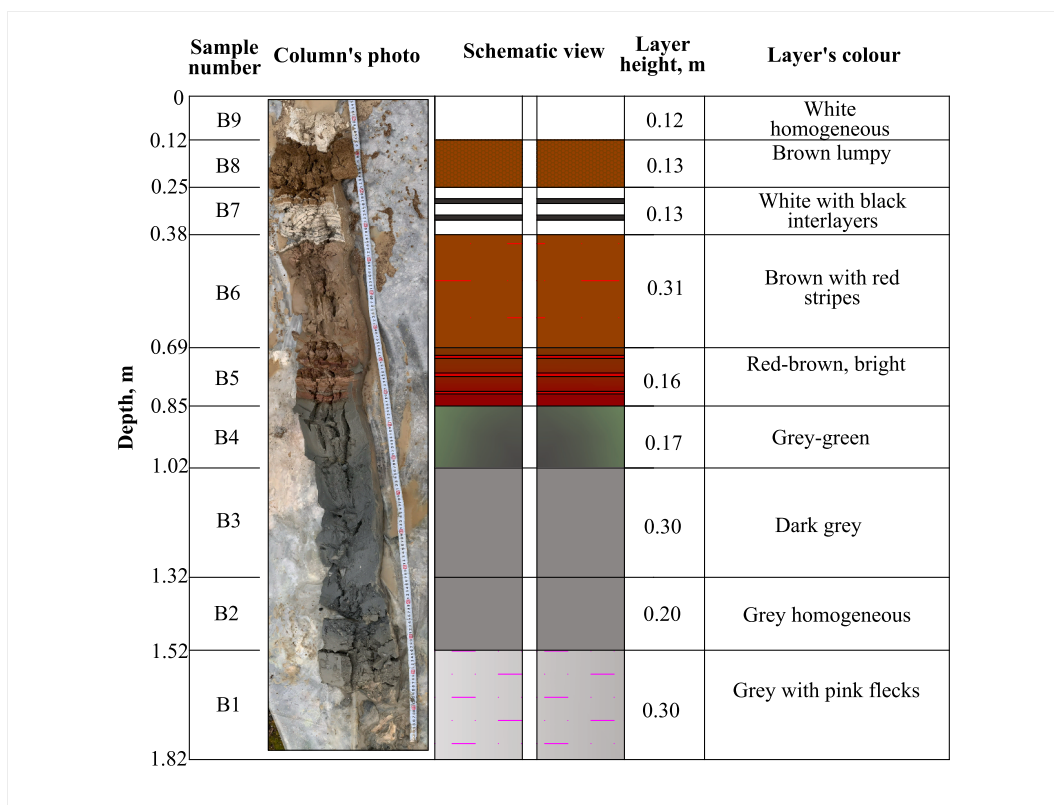

Sample number	Column's photo	Schematic view	Layer height, m	Layer's colour
B9			0.12	White homogeneous
B8			0.13	Brown lumpy
B7			0.13	White with black interlayers
B6			0.31	Brown with red stripes
B5			0.16	Red-brown, bright
B4			0.17	Grey-green
B3			0.30	Dark grey
B2			0.20	Grey homogeneous
B1			0.30	Grey with pink flecks

Depth, m: 0, 0.12, 0.25, 0.38, 0.69, 0.85, 1.02, 1.32, 1.52, 1.82

Fig. 3. Sediment section along the column B.

Table 1

Composition of the water extract from the columns.

	pH	TA	Cl⁻	SO₄²⁻	NO₂⁻	NO₃⁻	Ca²⁺	Mg²⁺	Na⁺	K⁺	OP	OS	Water content
		mg-eq/L	mg/kg									%	%
Column A													
A9	11.18	11.00	24,475	4,922	0.75	<3	13,335	225	5,610	347	479	1.72	44.0
A8	11.52	38.40	64,850	991	3.40	50.7	12,940	3.49	20,350	12,584	273	3.07	70.7
A7	11.55	33.00	58,250	6,195	1.91	355	13,088	416	21,985	16,408	354	3.39	69.8
A6	11.59	41.20	48,225	2,318	4.30	34.9	9,200	<1	18,545	15,108	142	3.65	69.7
A5	11.28	10.30	65,500	11,575	3.90	56.8	8,887	216	29,046	26,134	229	3.32	77.5
A4	11.20	8.32	84,050	13,203	9.10	61.7	1,960	765	33,632	29,447	418	3.35	79.6
A3	11.19	9.40	61,250	17,020	6.50	30.8	4,336	573	30,168	25,332	469	3.97	78.3
A2	11.21	10.50	57,650	15,198	0.56	18.7	4,387	1,084	29,550	23,455	374	4.22	76.1
A1	11.40	15.80	64,850	10,520	0.56	554	3,951	899	26,934	19,963	558	5.33	75.7
Column B													
B9	10.48	0.94	46,270	5,353	0.51	<3	16,936	1,308	9,611	226	204	3.04	51.3
B8	10.57	1.32	93,000	7,823	1.05	862	42,137	386	16,863	616	164	4.23	66.6
B7	10.33	0.84	46,735	3,764	0.50	<3	18,215	218	9,785	289	322	3.19	58.1
B6	10.44	1.18	92,800	4,548	0.33	27.9	35,078	441	26,350	1080	250	4.15	79.5
B5	10.32	1.12	114,600	3,002	0.58	<3	35,125	4,510	39,078	14,475	305	4.18	84.8
B4	10.37	1.06	85,500	4,872	0.18	29.7	33,808	1,007	21,000	892	547	5.08	79.4
B3	10.35	1.04	67,750	4,696	0.18	40.7	26,105	2,013	16,256	678	1075	5.30	77.5
B2	10.18	0.87	70,150	4,267	0.36	35.2	25,904	1,576	19,464	754	285	4.69	78.5
B1	9.89	0.61	76,775	4,953	0.17	31.6	26,243	1,739	19,293	891	549	5.94	78.4
p-value	<0.001	<0.001	0.064	0.112	0.002	0.200	<0.001	0.034	0.158	0.005	0.860	0.133	0.402

Note: TA – total alkalinity, OP – oil products, OS – total content of organic substances; Ammonium ions (NH_4^+) were not detected in the samples, p-value – the significance level of differences between columns A and B based on the Mann-Whitney test.

lower absolute pH range of 9.9–10.6. The total alkalinity of the B-column sludge was relatively low, ranging from 0.6 to 1.2 mg-eq/L.

The composition of the water extract of the upper A9 sludge was sodium-calcium chloride. As the depth increased, the amount of dissolved calcium dropped, but the amount of sodium and potassium increased. In some layers, the composition of the extract was calcium-sodium chloride and even potassium-calcium-sodium chloride. All layers had a high concentration of chloride, ranging from 48 to 84 g/kg, except for layer A9, where the chloride content was considerably lower (24 g/kg). The sulphate content ranged from 1 to 17 g/kg, with the highest values found in the lower A1–A5 layers. The content of nitrogen compounds was minimal. The total amount of organic compounds in column A increased with depth, while the colour of the sediment layer changed to black, and the samples developed a petroleum odour.

The water extracts of all B-column layers had a sodium-calcium chloride composition. All layers had a high chloride content ranging from 46 to 115 g/kg. The highest amounts were found in layers B8 and B4–B6, while the lowest content was observed in the surface layer B9. The sulphate content was nearly consistent across the profile, with the highest concentration found in the B8 layer. The nitrogen compound content was minimal.

Calcium was found primarily in the cationic fraction (17–42 g/kg), with the lowest concentrations in the upper layers B7 and B9. The second most major cation was sodium (10–39 g/kg), which was also lower in layers B7 and B9. Magnesium content ranged from 0.2 to 4.5 g/kg, and potassium content ranged from 0.2 to 1.1 g/kg, with layer B5 having the greatest concentration (14.5 g/kg).

Layer B3 contained the highest concentration of oil products (1.1 g/kg), while the other layers had a lower oil product content (0.2–0.5 g/kg). The content of organic matter increased from 3.0 % to 5.9 %; the highest concentrations were found in the lower layers (B1–B4).

The content of the eight most common environmental toxicants was assessed (Table 2). ICP-MS results were compared to Grogoriev's clark [44] for sedimentary rocks. Both columns had very high chromium, copper, lead, and mercury concentrations compared to the geochemical background of the sedimentary rocks.

The sludge composition analyses indicated differences between columns A and B. Principal Component Analysis (PCA) in R was used to depict differences in sludge composition between the columns in terms of anion, cation, and toxic trace element content. The first and second axes explain 54.4 % of the observed variance (31.9 % and 22.5 %, respectively) (Fig. 4).

The Mann-Whitney test revealed major differences ($p < 0.05$) between the samples from columns A and B in terms of the content of calcium, magnesium, potassium, and nitrite anions, as well as pH and total alkalinity (Table 1). These indicators showed the biggest variation in the chemical composition of the sediments in the studied columns. Between columns A and B, there were no considerable differences in the amounts of toxic trace elements ($p > 0.05$). Appendix 1 (Figs. S2.1-S2.21) shows boxplots with a comparison of chemical parameters in columns A and B.

The hierarchical cluster analysis of sediments' chemical composition found three clusters: column A layers, column B layers, and upper sludge layers (modern sediments) (Fig. 5).

3.4. Taxonomic profiles of microbial communities

The microbial community structure of the technogenic alkaline lake sediments was investigated using 16S rRNA gene amplicon sequencing on the Illumina MiSeq platform. The amplicon sequencing data were deposited at NCBI SRA as BioProject PRJNA1072311.

Table 2
The toxic trace elements in sludge.

|	Content, ppm							
	Cr	Co	Ni	Cu	Zn	As	Pb	Hg
Column A								
A9	68.80	6.93	18.10	45.78	12.20	2.56	79.27	1.08
A8	192.43	6.27	12.04	149.71	9.16	0.29	43.76	0.17
A7	1,225.45	8.05	16.32	772.59	17.01	1.17	309.80	0.27
A6	178.08	56.44	12.39	215.99	12.17	2.98	66.95	0.36
A5	1,753.96	21.26	56.30	3,397.72	47.82	4.62	218.99	1.94
A4	1,393.48	18.62	59.40	2,766.33	33.54	2.10	138.25	8.30
A3	1,561.36	17.19	37.93	1,331.79	38.87	5.11	168.66	1.76
A2	1,000.99	15.72	31.22	987.90	36.08	4.68	124.38	2.19
A1	725.26	18.40	38.68	1,149.03	33.98	8.49	109.16	4.50
Column B								
B9	140.98	7.90	9.98	1,513.85	10.47	3.01	144.27	0.17
B8	2,268.98	10.06	21.22	1,447.29	26.61	4.25	132.83	0.18
B7	47.66	1.59	2.17	9.51	2.11	0.57	13.02	0.11
B6	1,425.71	18.36	38.56	1,975.03	29.96	4.02	144.86	1.90
B5	491.38	9.23	57.55	3,763.57	21.98	2.75	59.04	7.71
B4	1,152.39	15.13	33.10	1,177.46	33.96	3.07	147.69	2.10
B3	952.00	10.28	32.73	1,156.64	41.78	7.68	140.79	2.66
B2	917.09	17.49	31.39	1,026.77	36.91	6.08	134.48	2.56
B1	1,120.89	12.33	34.65	1,161.30	35.08	3.74	155.53	2.59
Average content in sedimentary rocks [44]	**92.40**	**17.00**	**50.00**	**39.00**	**75.00**	**5.60**	**17.00**	**0.07**
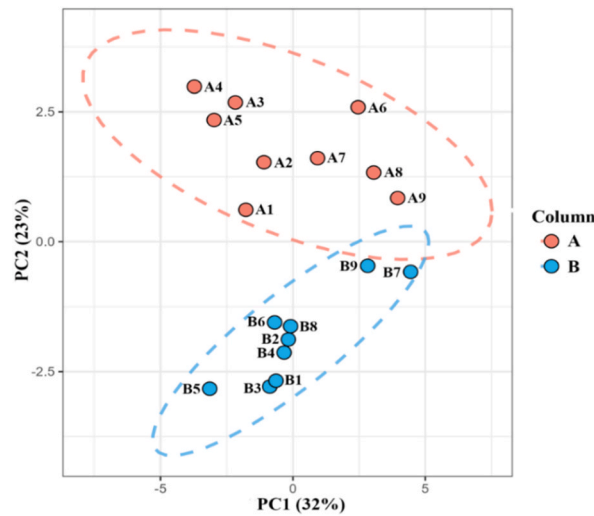
Fig. 4. Parameters of the chemical composition of sludges in columns A and B in the principal component graph.

Following filtration and denoising, 217,467 quality reads were obtained from 18 sediment samples. The average number of reads per sample was 12,653 (ranging from 8,339 to 16,898). These reads generated a total of 1280 unique ASVs.

A 16S rRNA gene-based metagenomic analysis found 29 phyla within the *Archaea* (2 phyla) and *Bacteria* (27 phyla) domains. Fig. 6 summarises the phylogenetic analysis of microbial communities found in sediments at phylum and class levels. *Proteobacteria* were the most prevalent phyla in all samples (61.19–84.25 %), followed by *Firmicutes* (7.67–19.21 %), *Actinobacteria* (3.34–13.28 %), *Bacteroidetes* (1.37–5.83 %), *Fusobacteria* (0.1–1.12 %), and *Cyanobacteria* (0.1–5.48 %). Other phyla with a relative abundance <1 % included *Chloroflexi*, *Acidobacteria*, *Verrucomicrobia*, *Planctomycetes*, *Chlorobi*, *Nitrospirae*, *Spirochaetes*, *Tenericutes*, and *Gemmatimonadetes*.

The top five bacterial classes included *Betaproteobacteria* (13.18–54.54 %), *Gammaproteobacteria* (15.42–37.79 %), *Alphaproteobacteria* (8.33–17.17 %), *Bacilli* (15.29–14.29 %), and *Actinobacteria* (3.1–13.12 %) (Fig. 6b). Dominant bacterial orders included *Burkholderiales* (11.44–53.93 %), followed by *Pseudomonadales* (13.58–35.34 %), *Actinomycetales* (3.1–13.12 %), *Lactobacillales* (3.48–10.36 %), *Rhizobiales* (4.27–10.91 %), *Bacillales* (2.19–5.90 %), *Clostridiales* (1.47–6.37 %), and *Caulobacterales* (0.97–5.88 %). The dominant bacterial genera included *Ralstonia* (8.95–52.88 %), *Pseudomonas* (10.70–33.19 %), *Streptococcus* (2.61–8.79 %), and *Bradyrhizobium* (1.72–10.29 %) (Fig. S3).
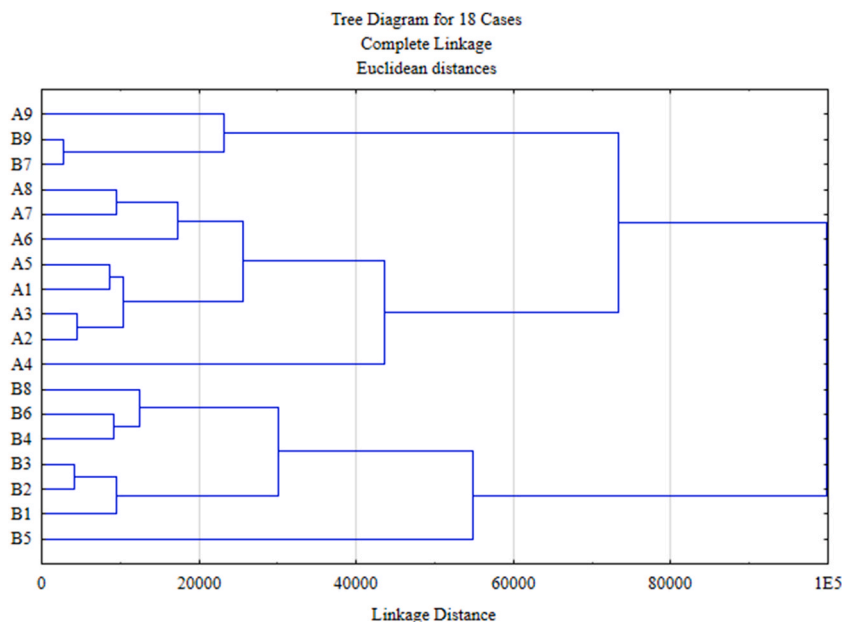

Fig. 5. Dendrogram of hierarchical cluster analysis of chemical composition parameters by sludge layers.
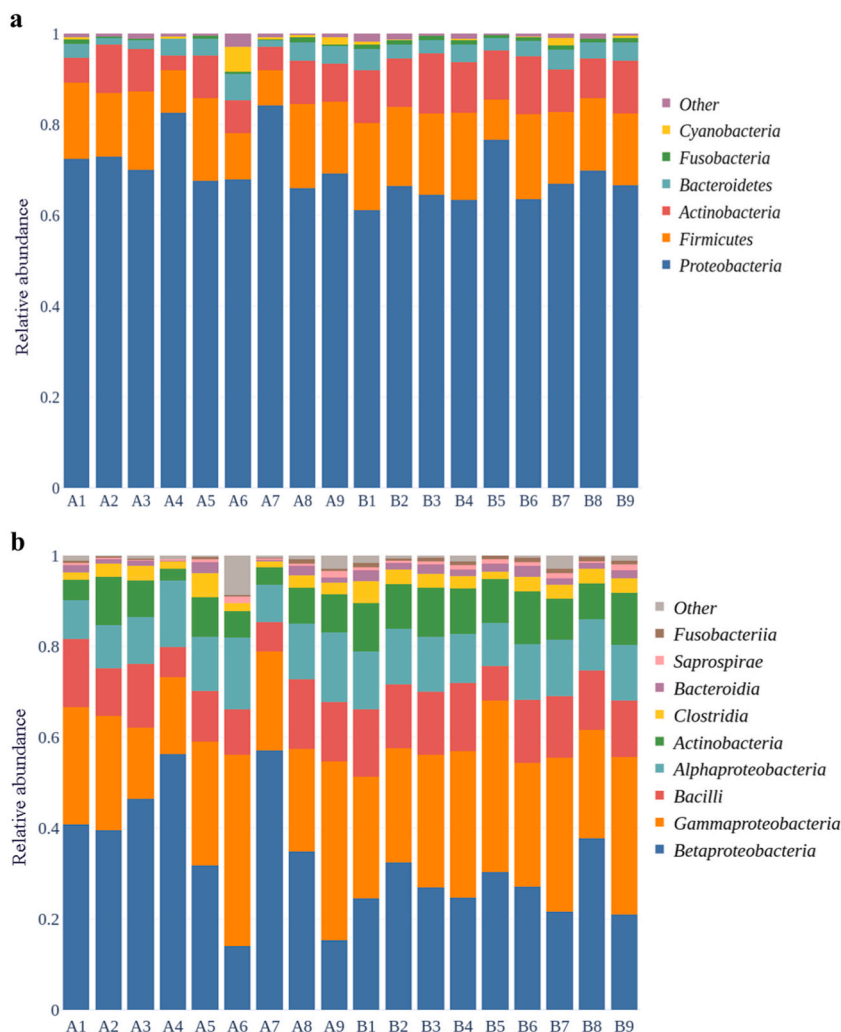
Fig. 6. The relative abundance of prokaryotic microorganisms at the phylum (a) and class (b). Groups occupying less than 1 % of the distribution were grouped together and designated as "Other".

Among the archaea, only two phyla were identified: *Euryarchaeota* and *Crenarchaeota* (relative abundance <1 %). Representatives of these phyla belong to the genera *Nitrosomonas* and *Nitrososphaera*. Archaea were found in column B, specifically in samples B8, B1, and B2, which might indirectly suggest that archaea were more abundant in the deeper sediment layers.

The phylum *Proteobacteria* is the most abundant in column A (72.52 %), with the highest relative content in samples A4 (depth intervals of 0.93–1.04 m) and A7 (depth intervals of 0.42–0.51 m) (Fig. 6a). The phylum *Proteobacteria* was represented by three main classes: *Betaproteobacteria* (13.18–54.54 %), *Gammaproteobacteria* (15.42–37.78 %), and *Alphaproteobacteria* (8.33–17.17 %). Among the classes, *Betaproteobacteria* prevailed in all samples except for A6 and A9, where the relative content of *Betaproteobacteria* was nearly half that of *Gammaproteobacteria* (Fig. 6b).

In sample A5, a nearly similar content of *Betaproteobacteria* (30.17 %) and *Gammaproteobacteria* (25.7 %) was found. The class *Betaproteobacteria* was mainly composed of the order *Burkholderiales*, the family *Oxalobacteraceae*, and the genus *Ralstonia* (Fig. 6b). Among the representatives of *Gammaproteobacteria*, *Pseudomonadales* was the most prevalent, with the genus *Pseudomonas* being more abundant. Furthermore, the genera *Streptococcus*, *Bradyrhizobium*, *Brevundimonas*, *Propionibacterium*, *Acinetobacter*, *Staphylococcus*, *Sphingomonas*, and *Corynebacterium* were highly present (Fig. S3).

Cyanobacteria were more prevalent in sample A6 (5.48 %) compared to the other samples (Fig. 6a), while chemical analysis of this particular sample showed a relatively low concentration of Mg^{2+}, K^+, Na^+, and Cl^- ions (Table 1), as well as a lower content of heavy metals (Table 2). The *Cyanobacteria* were represented by the families *Synechococcaceae*, *Pseudanabaenaceae*, *Phormidiaceae*, and *Xenococcaceae*. In comparison to the other samples, sample A6 generally had a greater variety of families and genera. Sample A4 stood out due to its low abundance of *Actinobacteria* (3.09 %) and a relatively high content of *Flavobacteria* (2.42 %), which did not exceed 1 % in the other samples. *Flavobacterium* was the most prevalent genus (2.42 %) in the *Flavobacteria* class. *Ralstonia* (50.01 %), *Pseudomonas* (11.46 %), and *Bradyzhizobium* (10.29 %) were the tree most prevalent genera in this particular sample (Fig. S3).

Proteobacteria prevailed in columns B and A (66.57 %) (Fig. 6a). Within this phylum, the three main representative classes were *Betaproteobacteria* (20.21–35.14 %), *Gammaproteobacteria* (22.03–29.40 %), and *Alphaproteobacteria* (9.39–12.69 %) (Fig. 6b). These classes were almost equally represented, unlike in column A, where *Betaproteobacteria* predominated over *Gammaproteobacteria*, except in sample B8, where the amount of *Betaproteobacteria* (35.14 %) was nearly double the amount of *Gammaproteobacteria* (22.03 %). In comparison to column A, column B displayed a higher relative abundance of the *Actinobacteria* (8.76–14.69 %), represented by *Propionibacterium* (1.96–3.27 %), *Corynebacterium* (1.27–2.9 %), *Actinomyces* (1.36–2.21 %), and *Rothia* (0.44–2.09 %) (Fig. 6b, Fig. S3).

The relative abundance of *Cyanobacteria* in sample B7 was higher (1.51 %) compared to the other samples from column B (Fig. 6a), with low concentrations of Mg^{2+}, K^+, Na^+, and Cl^- (as in A6). In sample B5, *Proteobacteria* prevailed (77 %) and were represented by *Ralstonia* (27.62 %), *Pseudomonas* (29.92 %), *Bradyrhizobium* (5 %), *Brevundimonas* (1.38 %), *Acinetobacter* (0.77 %), *Sphingomonas* (1.59 %), and several other genera (Fig. S3). The percentage of *Firmicutes* was found to be 8.96 %, which is lower than the percentage in the other samples from column B (15.81–19.21 %).

3.5. The impact of environmental factors on microbial communities

RDA was conducted to reveal the connection between microbial community structure and environmental variables. Chemical variables underwent a VIF test prior to the analysis because collinearity among variables can introduce uncertainty into the RDA results. Chemical variables that exhibited a high VIF value and strong collinearity were excluded from the analysis. Therefore, the analysis used eight chemical variables that complied with the RDA.

According to the RDA analysis, the samples were grouped in columns A and B, suggesting that the microbial community structure in the two columns was distinct. This finding was further supported by the PCoA (Fig. 7a). The distribution of the microbial community was influenced by the geochemical features of the sampling sites (columns A and B). All data followed geochemical trajectories from K^+-rich to Ca^{2+} and Mg^{2+}-rich conditions, as well as from more alkaline to less alkaline conditions (Fig. 7a).

The RDA biplot indicated that distinct chemical variables affected the distribution and composition of microbial communities in bottom sediments. The results of the bacterial RDA (Fig. 7) showed that the first two axes explained 21.67 % and 17.39 %, respectively, of the total variation. Among environmental variables, Ca^{2+}, K^+, and TA (total alkalinity) were found to be the most influential factors and exhibited a considerable correlation with microbial communities in the two columns of bottom sediments in an alkaline reservoir ($p < 0.05$).

The diversity of the microbial community also relied on the concentrations of Mg^{2+} (13.8 %, p = 0.023) and Cr (12.32 %, p = 0.04).
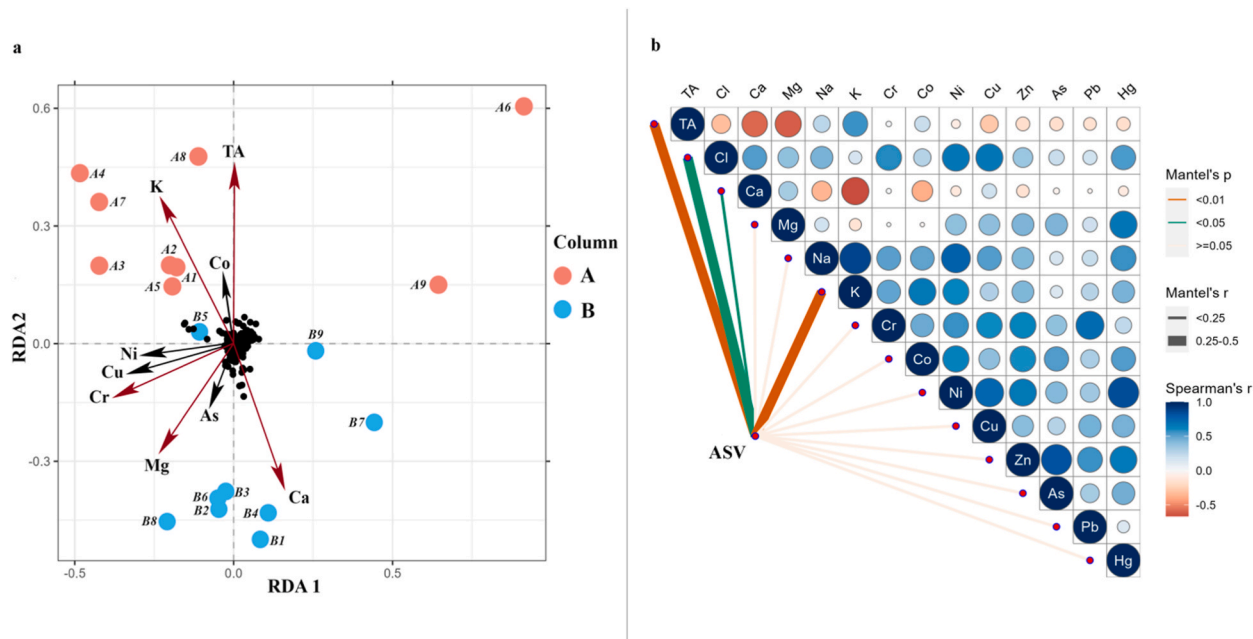

Fig. 7. Environmental drivers of microbial community composition. a) RDA ordination showing the microbial community composition in relation to environmental variables. The direction of the arrow indicates a positive or negative correlation among the environmental factors with the ordination axes. The length of the arrow reflects the strength of the correlation between environmental factors and the variability of microbial communities (long lines indicate a strong correlation). The red arrows indicate factors that have a considerable correlation; b) the microbial community is related to each environmental factor by partial Mantel test (edge width corresponds to the Mantel's r statistic for the corresponding distance correlations, and the edge colour denotes the statistical significance based on 9999 permutations). (For interpretation of the references to colour in this figure legend, the reader is referred to the Web version of this article.)

In column A, there was a positive correlation between the values of K$^+$, TA, and microbial diversity, while column B exhibited the opposite correlation.

The microbial community structure in column B was more affected by Mg^{2+} and Ca^{2+} than other environmental factors. Other environmental factors (Co, Ni, Cu, and As) showed a weak correlation with the microbial communities (p > 0.05).
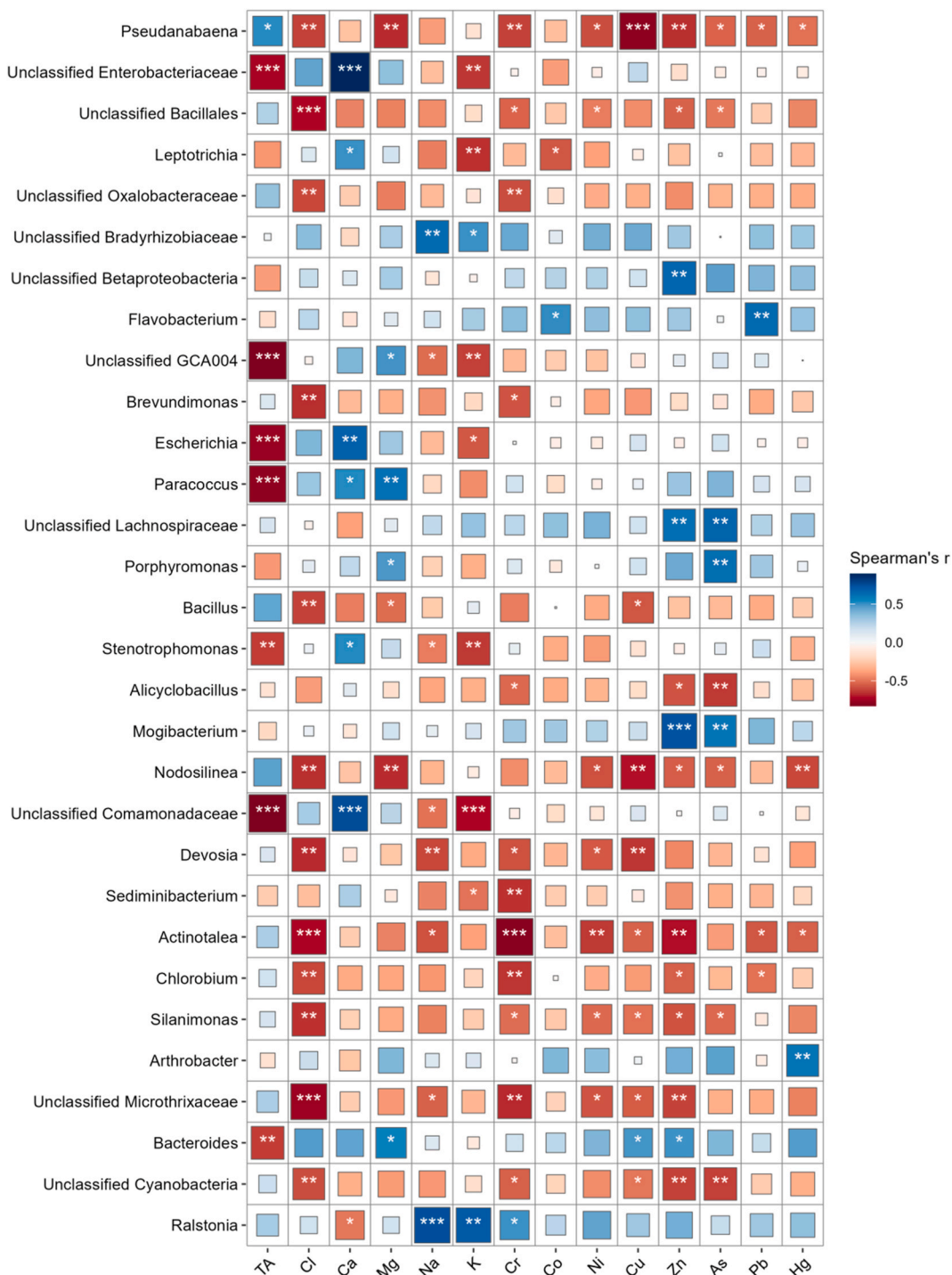

Fig. 8. Heatmap of correlations between microbial genus and environmental variables (the R value is displayed in different colours, (*) p-value ≤0.05; (**) p-value ≤0.01; (***) p-value ≤0.001). (For interpretation of the references to colour in this figure legend, the reader is referred to the Web version of this article.)

The Mantel test confirmed the discovered patterns. Fig. 7b shows a substantial correlation between TA, K$^+$ (Mantel >0.25, p < 0.01), and microbial community structure. Ca^{2+} and Cl$^-$ (Mantel <0.25, p < 0.05) were also important factors for the microbial community.

Spearman's rank correlation test (Fig. 8, Fig. S4) was done to explain the connection between environmental factors and prokaryotic composition (relative abundance at the phylum and genus).

The most prevalent phylum, *Proteobacteria*, showed a positive correlation with TA and K$^+$ (p-value <0.01). The graph (Fig. S5) shows that column A, which has high TA and K$^+$ values, contains a much higher portion of *Proteobacteria* than column B.

Contrary to *Proteobacteria, Actinobacteria* exhibited a negative correlation with TA but a positive correlation with Ca^{2+} and Mg^{2+}. *Bacteroidetes*, *Chloroflexi*, and *Cyanobacteria* had a negative correlation with Na$^+$. *Cyanobacteria* and *Chlorobi* were negatively correlated with toxic trace elements (Cr, Ni, Cu, Zn, and As, in particular). It should be noted that no significant difference was found between columns A and B in terms of toxic element content and the number of *Cyanobacteria* and *Chlorobi*. However, the graph displaying *Cyanobacteria* and *Chlorobi* (Figs. S6 and S7) in different sludge layers shows that in the layers with relatively low toxic element content (A6, A9, and B7), the number of *Cyanobacteria* and *Chlorobi* phyla representatives is much higher than in the remaining samples, where the heavy metal content is several times higher.

At the genus level, a negative correlation (p-value <0.001) was observed between the content of Cl$^-$, Mg^{2+}, Cr, Cu, Zn and the abundance of bacteria of the genera *Pseudanabaena* and *Nodosilinea* (phylum *Cyanobacteria*) (Fig. 8). We also observed a strong negative correlation between total alkalinity and the abundance of representatives of the families *Comamonadaceae* (r = −0.83, p-value = 2.19E-05), GCA004 (r = −0.83, p-value = 2.28E-05), genera *Escherichia* (r = −0.76, p-value = 0.00022) and *Paracoccus* (r = −0.78, p-value = 0.00012). In addition, a positive correlation was found between Ca^{2+} content and the representatives abundance of the families *Comamonadaceae* (r = −0.75, p-value = 0.00036) and *Enterobacteriaceae* (r = −0.90, p-value = 5.32E-07), in particular the genus *Escherichia*. The abundance of representatives of the genus *Actinotalea* (phylum *Actinobacteria*) was negatively correlated with Cl$^-$ content and concentrations of heavy metals (Cr, Ni, Zn) (Fig. 8).

3.6. Alpha diversity of microbial communities

The results of the alpha diversity analyses showed that the microbial community's richness (the Chao1 index), diversity (the Shannon index and Simpson index), and equitability (Pielou's evenness) differed between samples (Table 3, Fig. 9). Layers A6 and B5 were found to have the highest and lowest species richness, respectively.

In order to assess the microbial diversity in each sample of sludge, the sequencing results were grouped based on column distributions. The species richness (Chao1) of the two columns' microbial communities did not differ considerably (p = 0.49, Kruskal-Wallis H test). Column A appeared to have lower community equitability as indicated by Pielou's evenness values (p = 0.004, Kruskal-Wallis H test). As a result, column B had much higher Simpson and Shannon indices than column A (p = 0.019 [Simpson], p = 0.063 [Shannon], Kruskal-Wallis H test). These indices reflect both community richness and evenness.

3.7. Microbial community structure

In this study, PERMANOVA analysis was used to see if there were any considerable differences in microbial composition between columns A and B, as well as between different layers of bottom sediments. Additionally, PCoA plots from Bray-Curtis dissimilarity were used to distinguish microbial diversity between the columns. Principal coordinate analysis (PCoA) plots for beta diversity were generated using the phyloseq package in R. As shown in the PCoA, the samples were divided into two groups based on column distribution, which can be attributed to differences in environmental factors. The first two principal coordinates accounted for 45.6 % of

Table 3
Alpha indices of microbial communities in sludges.

| Samples	Chao1	Shannon	Simpson	Coverage	Pielou's Evenness
A9	147	4.03034	0.96441	1.0	0.80761
A8	114	3.85307	0.96275	1.0	0.81354
A7	131	3.18810	0.91695	1.0	0.65394
A6	225	4.44428	0.97523	1.0	0.82124
A5	158	4.01672	0.96591	1.0	0.79441
A4	135	3.22388	0.91586	1.0	0.65723
A3	159	3.72226	0.94509	1.0	0.73433
A2	118	3.66795	0.95165	1.0	0.77023
A1	136	3.78447	0.95515	1.0	0.77151
B9	144	4.11317	0.97092	1.0	0.82763
B8	111	3.89218	0.96462	1.0	0.82645
B7	157	4.23701	0.97516	1.0	0.83903
B6	112	4.04130	0.97340	1.0	0.85811
B5	84	3.49985	0.95135	1.0	0.79203
B4	128	4.10793	0.97446	1.0	0.84664
B3	121	4.03481	0.97196	1.0	0.84132
B2	164	4.07206	0.96880	1.0	0.80136
B1	172	4.34552	0.97807	1.0	0.84420
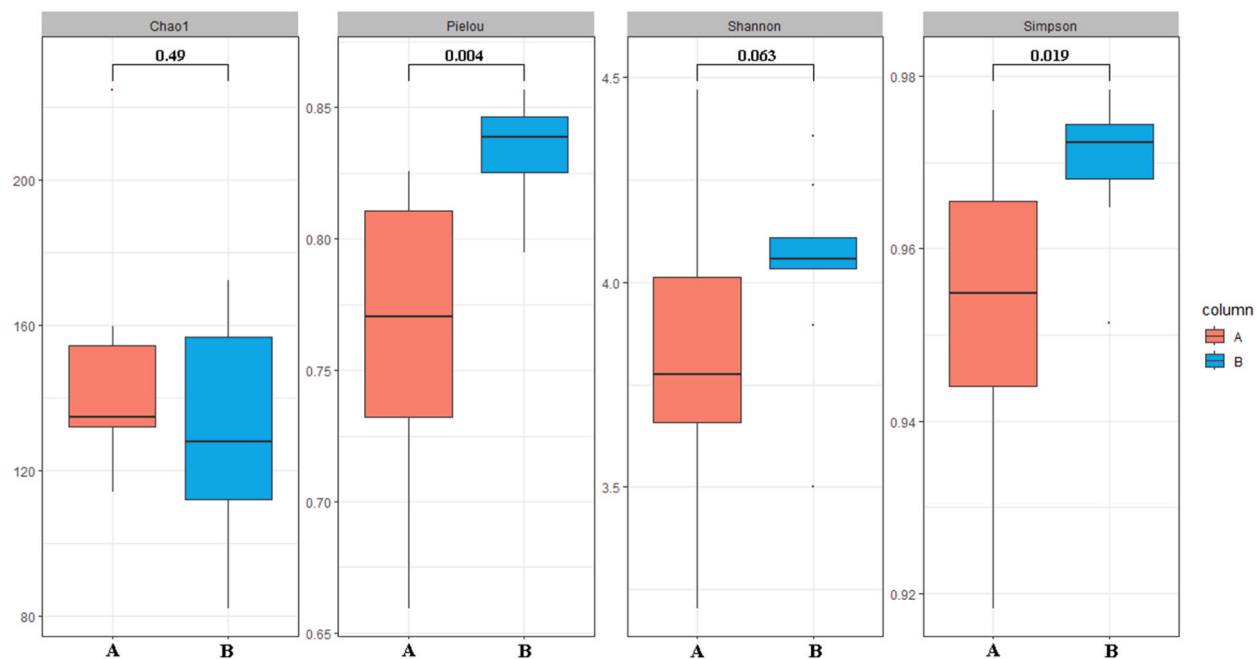
Fig. 9. Microbial biodiversity in the two columns of bottom sediments of a saline alkaline technogenic reservoir: α-diversity was indicated by Chao1 index (a measure of richness), Pielou's evenness (a measure of equitability of community structure), Shannon index (a measure of both richness and evenness), and Simpson index. Data used for alpha diversity calculations were normalised by randomly sub-sampling 8,339 sequences in each sample to minimise the effects caused by different sequencing efforts.

the total variation (Fig. 10). PERMANOVA analysis revealed a notable difference in biodiversity between columns A and B (PER-MANOVA, P < 0.001).

The boxplot (Fig. 11b) depicts the distance pairings of samples between the columns and shows that the dissimilarity of the samples in columns A and B is significant, which is consistent with the PERMANOVA results.

The data in columns A and B are clearly clustered together in the heatmap (Fig. 11a). At the same time, layer 6 has a higher Bray-Curtis dissimilarity index than any other sample. The highest species richness and diversity were also noted in this layer.

The differences in sediment chemistry between columns A and B shown above are also visible in the structure of the microbial communities when beta diversity is taken into account. However, PERMANOVA analysis showed no considerable difference between the microbial communities in different sediment layers (A1–A9, B1–B9) (PERMANOVA, P > 0.05).
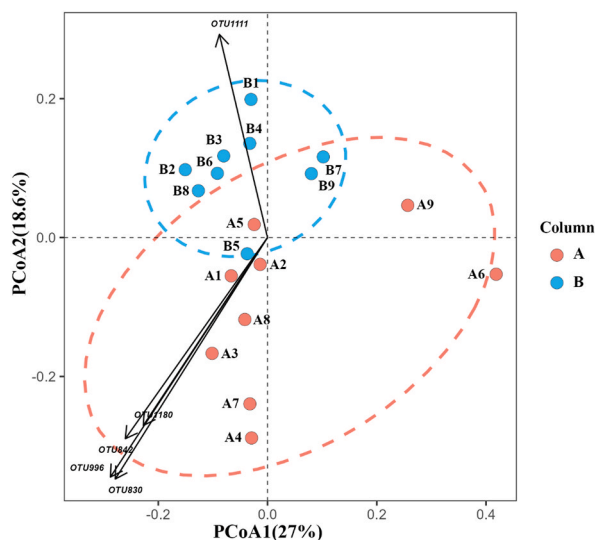

Fig. 10. Principal coordinate (Bray-Curtis) plot showing the β-diversity of bacterial community.

Linear discriminant effect size (LEfSe) analysis was conducted to find and compare the distinct microbial taxa associated with each column of bottom sediments. LDA results were assessed after cladograms depicted the biomarker bacterial groups. Fig. 12 shows the taxa for each column. *Enterobacteriaceae, Comamonadaceae,* and *Rhodobacteraceae* were represented by the indicator bacteria in column B. These results were also confirmed by ANCOM (Fig. S8).

PERMANOVA was used to compare samples with the highest (A4, A5, B5) and lowest (A9, A7, A6) concentrations of toxic elements to determine whether or not heavy metals are a significant factor in the formation of microbial communities. PERMANOVA revealed a considerable difference between the microbial communities in samples rich in heavy metals and samples low in toxic elements (p = 0.0015). For both groups, LEfSe was used in order to identify indicator species (LDA >4). LEfSe (Fig. 13) revealed the indicator families for samples with high amounts of toxic elements: *Burkholderiaceae* (genus *Ralstonia*), *Oxalobacteraceae*, and *Bradyrhizobiaceae*. Representatives of the phylum *Cyanobacteria*, orders *Caulobacterales* and *Bacillales* as well as the genus *Campylobacter* were biomarker microorganisms in samples with low concentrations of heavy metals. Negative correlation of the phylum *Cyanobacteria* was found using correlation analysis (Fig. S4.).

4. Discussion

Proteobacteria, Firmicutes, and *Actinobacteria* are the three bacterial phyla that make up the majority of the samples used in this study. They have a broad distribution and high metabolic flexibility, which suggests that they can withstand harsh environmental conditions and use various carbon compounds as energy sources [45,46]. The findings are in line with previous research, which has demonstrated that the *Proteobacteria, Firmicutes*, and *Actinobacteria* phyla are the most prevalent bacterial groups present in saline and alkaline environments all over the world [18,47,48]. These bacteria were found in natural soda ash lake ecosystems like Lake Van (Türkiye), Lonar Lake (India), and Lake Tanatar (Russia) [49–51], hypersaline soils and sediments [52,53], saline lakes, solonchaks, and salt mines [13], as well as in artificial habitats [18,21,22].

Ralstonia and *Pseudomonas* are the two most prevalent genera in the sediment samples. The genera *Ralstonia* and *Pseudomonas* have significant geochemical functions, as evidenced by earlier studies. These genera have previously demonstrated the ability to biodegrade aliphatic hydrocarbons [54,55], aromatic compounds [56,57], and phenolic compounds [58]. They also showed the ability to change a variety of nitrogen-containing substances [59,60]. Additionally, heavy metal resistance genes have been found in *Ralstonia* and *Pseudomonas*. There is a potential in using these organisms to bioremediate ecosystems that have been contaminated with toxic
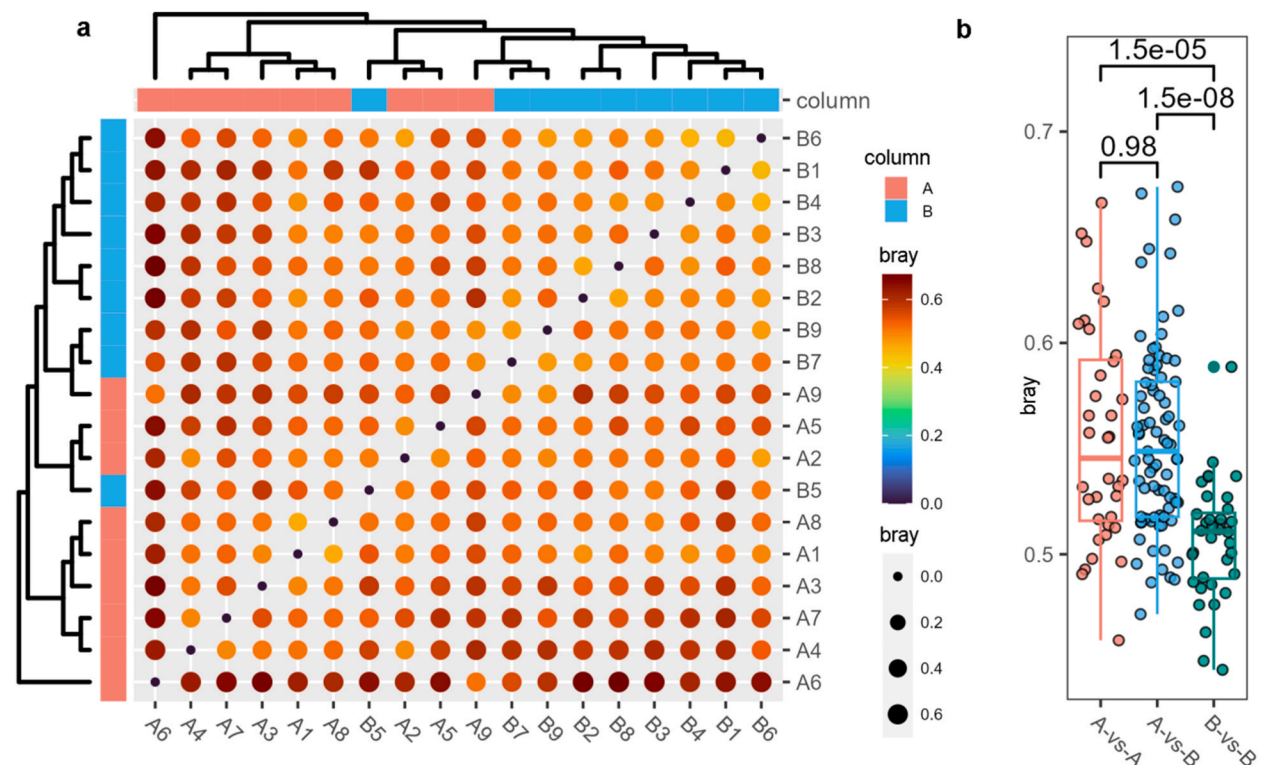

Fig. 11. The distribution pattern of microbial communities from the bottom sediments of an anthropogenic reservoir with saline alkaline water: a) Samples heatmap based on Bray-Curtis similarity of microbial community composition among all layers; b) the boxplot for each sample. The size and colour of the heatmap represent the distance of each sample, and colour of bar plot represents the group of the sample. (For interpretation of the references to colour in this figure legend, the reader is referred to the Web version of this article.)
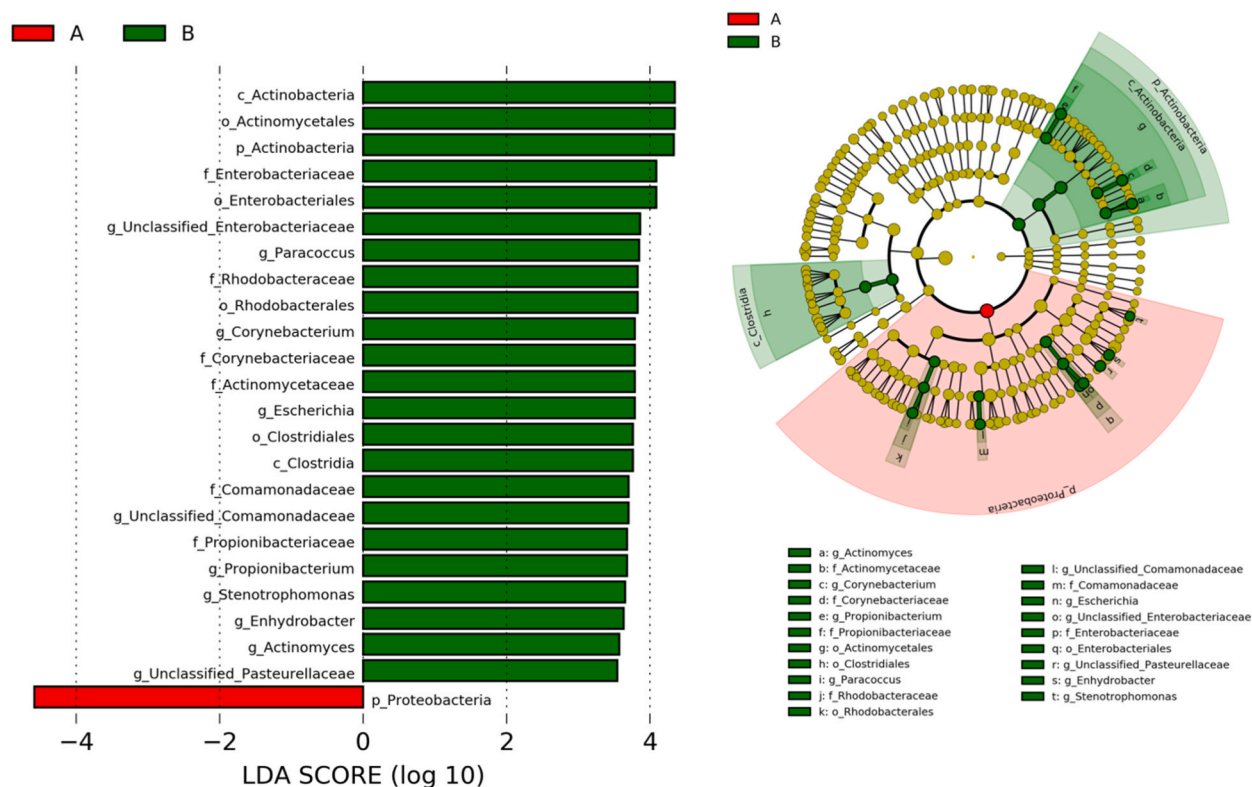
Fig. 12. LEfSe of microbial abundance between column A and column B samples.

inorganic elements (heavy metals) [61–63].

Low amounts of oxigenic (*Cyanobacteria*) and anoxigenic (*Rhodospirillales, Rhodocyclales, Rhodobacterales, Chlorobi,* and *Chloroflexi*) phototrophic bacteria were found in the samples. This may indicate that carbon is fixed in the technogenic lake by alternative ways. The relative abundance of methanotrophic bacteria (*Methylococcus*) was also found to be quite low. These bacteria may be involved in biogenic methane cycle in lake sediments.

The studied technogenic lake had a relatively high microbial diversity despite its extremely saline and alkaline conditions. We compared our data with previously published studies on both alkaline and saline soil [48] and saline and hypersaline lakes [13,53]. Our alpha diversity metrics at the ASVs level are relatively high (Table 3). The presence of layers with different structures and properties in lake sediments makes them a more heterogeneous habitat, which could be one explanation for the different results. Chemical and physical stratification in bottom sediment ecosystems enables the creation and maintenance of high diversity both within and between microbial communities [52,64]. Similar alpha diversity values have been found in microbial communities in sediments from La Sal del Rey [52], near the Mediterranean coast (France) [65] and salt mines [13,47]. However, alpha diversity values were relatively low [23] compared to data from anthropogenically polluted habitats with pH values between 7 and 8, as well as data from natural soda ash lakes [46,51].

We focused on the characteristics of the microbiota in various parts of the technogenic pond and at various depths when analysing the factors affecting the microbial community. The variety of effluents, coming in over a long period of time, contributed to the formation of distinct layers containing various main salt components (chloride ions, calcium, sodium, potassium) and toxic micro-elements. According to granulometric analysis, the precipitation of elements from solutions was the main factor of sediment formation. The outside particles contributed much less to the composition of the sludge.

The most considerable differences in the structure of microbial communities were found laterally (between columns A and B), not by depth (different sediment layers). The analysis of the taxonomic distribution of microbial groups in alkaline saline lake sediments also showed no significant differences in the depth of the studied layers (from the surface to the deepest layer). In contrast, the microbial diversity study of saline alkaline lime in storage ponds in Janikowo found distinct differences in the taxonomic composition of microbial communities between the surface layers and deep layers. The authors attribute this pattern to a decrease in salinity in the surface sediment layers, which suggests more favourable conditions for microorganisms to exist [18]. The average pH values and chloride ion concentrations are comparable to those obtained in the studied samples from columns A and B. The content of sodium ions in the columns is much lower than the average value found in Janikowo, while the content of calcium ions is much lower in the column A and much higher in the upper and middle layers of the column B (Fig. S9).

Salinity, alkalinity, and toxic element content are the key factors (among many others) that can determine how different the
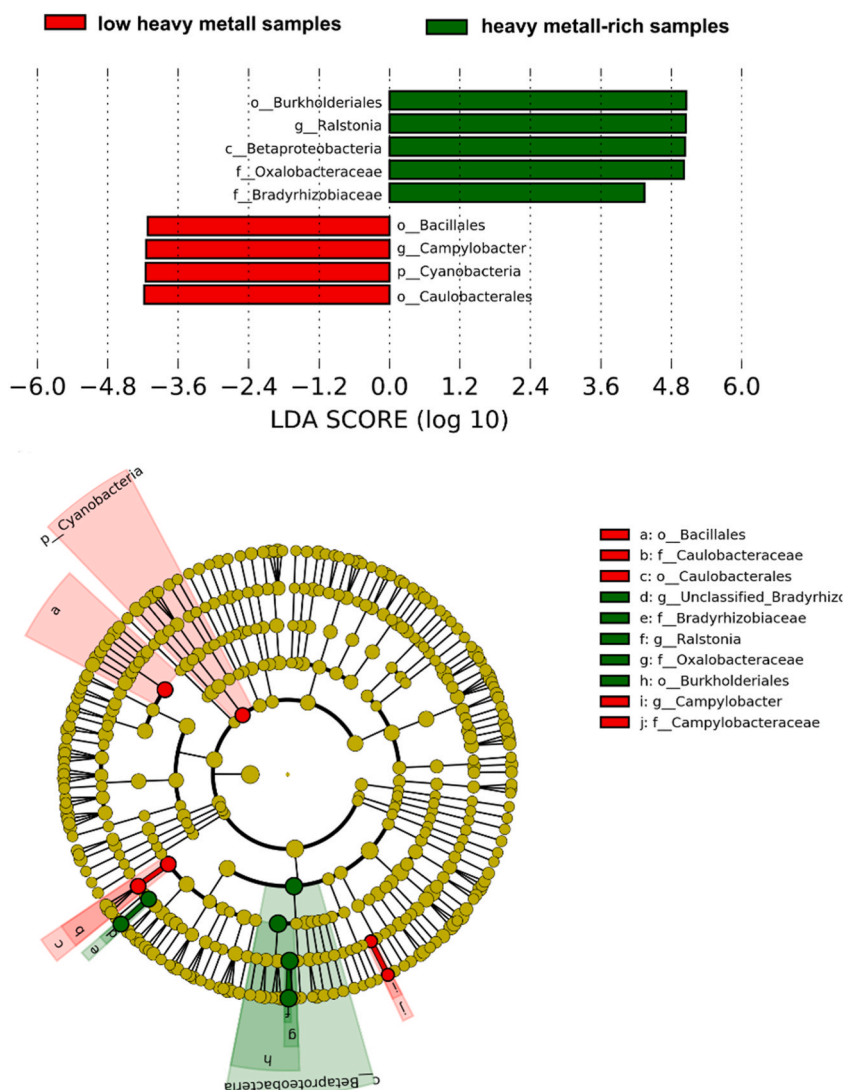
Fig. 13. LEfSe analysis of microbial abundance between samples rich in toxic metals and samples with low levels of toxic metals.

phylogenetic diversity of microbial communities in columns A and B is [18,21,66].

Numerous studies have examined how salinity and pH affect the composition and diversity of microbial communities in various ecosystems [18,52]. Compared to other environmental factors (pH, temperature, etc.), salinity has been found to be the key factor that determines the structure, composition, and metabolic activity of microbial communities, having a major impact on bacterial and archaeal communities [64]. Overall, the correlations described in this study also indicate that salinity (Cl^-, Na^+, and K^+) is an important factor affecting microbial communities in technogenic saline and alkaline lake sediments (Figs. 7 and 8). Similar trends were observed when saline alkaline lime was studied in storage ponds in Janikowo [18].

Total alkalinity was the key factor in this study, along with salinity, in affecting the composition of the microbial communities. Wastes from the production of potent alkalis and acids were present in the lake's area near column A, as evidenced by its high pH, potassium concentrations, and overall alkalinity. The phylum *Proteobacteria* is the indicator taxon of sediments in column A, and it appears to be connected with the ability of these bacteria to exist in highly alkaline environments. *Actinomycetaceae, Enterobacteriaceae, Comamonadaceae,* and *Rhodobacteraceae* are much more abundant in column B. Apparently, technogenic and municipal pollutants along with salinity and alkalinity contribute to the formation of the microbial community in column B.

In contrast to metabolised organic pollutants, high levels of heavy metals (Co, Cu, Pb, and Hg) have a big influence on microbial communities [62], play a special role in the formation of microbial communities, and can be a limiting factor due to persistence, toxicity, and bioaccumulation. Comparison of the results from the analysis of toxic elements in columns A and B sediment layers to the results from the analysis of alkaline industrial alumina products [21] shows that the studied sediments are rich in heavy metals such as chromium, copper, and lead (Table 2, Fig. S10).

This study shows that the genus *Ralstonia* is an indicator species in the samples with the highest content of toxic elements in

comparison to the others. Their ability to function normally in these conditions can be used to explain the high relative abundance of *Ralstonia* and *Pseudomonas* in the examined sediment samples (as mentioned earlier). For other species, high concentrations of heavy metals appear to be a limiting factor.

It is worth noting that in the present study toxic metals were present in varying concentrations in all layers of the bottom sediments. Accordingly, they affected the microbial communities of all layers in some way. This fact does not allow us to determine exactly how heavy metals affect the structure of microbial communities. In this respect, it is interesting to analyse bottom sediments with similar physico-chemical parameters but not affected by heavy metals. Further research will also focus on the study of similar artificial habitats, their subsequent comparison and meta-analysis.

5. Conclusions

This study describes the structure and composition of bottom sediments of a salt-alkali water body of technogenic origin located on the territory of the Verkhnekamskoe Salt Deposit (Russia), based on the microbial community inhabiting it.

The bottom sediments of the reservoir have layers that vary by visual characteristics, chemical composition, and the amount of toxic trace elements. The study also found notable variations in sediment characteristics along the reservoir's lateral. These variations are attributed to previous sources of wastewater with different compositions.

The lack of obvious differences in the physico-chemical characteristics of the saline-alkali sediments within the studied columns may be the reason why analysis of the distribution of microbial taxonomic groups in the bottom sediments of the saline-alkali water body failed to reveal any significant differences in the depth of the layers examined. The majority of the bacteria in the samples are *Proteobacteria*, *Firmicutes* and *Actinobacteria*, which are common in saline and alkaline environments worldwide. However, differences were found in the phylogenetic diversity of the column microbial communities sampled from different parts of the technogenic water body.

The phylum *Proteobacteria* is the indicator taxon in column A. Its deposits are linked to the former inflow of the most alkaline effluents. Significantly more *Actinomycetaceae, Enterobacteraceae, Comamonadaceae,* and *Rhodobacteraceae* representatives were found in column B as a result of a decrease in alkalinity and an increase in the magnesium and calcium content. This research also revealed that *Ralstonia* is the indicator species in samples with the highest content of toxic elements in comparison to the others.

The findings can be used to retrace the inflow of wastewater of various compositions into water body in question. Such knowledge is necessary for proper reclamation planning. Furthermore, understanding which bacteria can survive in environments with high salinity, alkalinity, and toxic element content can be helpful in the development of biotechnological approaches to the treatment of hazardous waste.

Funding

Data availability statement

The fastq data have been deposited in the SRA BioProject database (https://www.ncbi.nlm.nih.gov/sra) with accession number PRJNA1072311.

CRediT authorship contribution statement

Pavel Belkin: Writing – review & editing, Writing – original draft, Project administration, Investigation, Funding acquisition, Formal analysis, Data curation, Conceptualization. **Yulia Nechaeva:** Writing – review & editing, Writing – original draft, Visualization, Software, Formal analysis, Data curation. **Sergey Blinov:** Writing – review & editing, Supervision, Resources, Methodology, Funding acquisition, Conceptualization. **Sergey Vaganov:** Writing – original draft, Resources, Investigation. **Roman Perevoshchikov:** Writing – original draft, Visualization, Resources, Investigation. **Elena Plotnikova:** Writing – review & editing, Validation, Methodology.

Declaration of competing interest

The authors declare that they have no known competing financial interests or personal relationships that could have appeared to influence the work reported in this paper.

Appendix A. Supplementary data

Supplementary data to this article can be found online at https://doi.org/10.1016/j.heliyon.2024.e33640.

References

[1] R. Han, X. Zhang, J. Liu, Q.F. Long, L.S. Chen, D.L. Liu, D.R. Zhu, Microbial community structure and diversity within hypersaline Keke Salt Lake environments, Can. J. Microbiol. 63 (2017) 895–908, https://doi.org/10.3390/microorganisms8010120.

[2] Y. Nogi, H. Takami, K. Horikoshi, Characterization of alkaliphilic Bacillus strains used in industry: proposal of five novel species, Int. J. Syst. Evol. Microbiol. 55 (6) (2005), https://doi.org/10.1099/ijs.0.63649-0.

[3] C.S. Oie, C.E. Albaugh, B.M. Peyton, Benzoate and salicylate degradation by Halomonas campisalis, an alkaliphilic and moderately halophilic microorganism, Water Res. 41 (6) (2007) 1235–1242, https://doi.org/10.1016/j.watres.2006.12.029.

[4] N. Solat, M. Shafiei, A novel pH and thermo-tolerant halophilic alpha-amylase from moderate halophile Nesterenkonia sp. strain F: gene analysis, molecular cloning, heterologous expression and biochemical characterization, Arch. Microbiol. 203 (6) (2021) 3641–3655, https://doi.org/10.1007/s00203-021-02359-7.

[5] P. Gómez Villegas, Metagenomic Characterization, Bioactive Properties and Biotechnological Applications of the Extremophilic Microorganisms Inhabiting Odiel Saltern Ponds (Doctoral Dissertation), 2021 hdl.handle.net/10272/20213.

[6] W.S. Shu, L.N. Huang, Microbial diversity in extreme environments, Nat. Rev. Microbiol. 20 (2022) 219–235, https://doi.org/10.1038/s41579-021-00648-y.

[7] G.S. Roadcap, R.A. Sanford, Q. Jin, J.R. Pardinas, C.M. Bethke, Extremely alkaline (pH > 12) ground water hosts diverse microbial community, Ground Water 44 (4) (2006) 511–517, https://doi.org/10.1111/j.1745-6584.2006.00199.x.

[8] J.H. Jacob, E.I. Hussein, M.A.K. Shakhatreh, C.T. Cornelison, Microbial community analysis of the hypersaline water of the Dead Sea using high-throughput amplicon sequencing, Microbiology open 6 (5) (2017) e00500, https://doi.org/10.1002/mbo3.500.

[9] J. Pollock, K.A. Weber, J. Lack, L.A. Achenbach, M.R. Mormile, J.D. Coates, Alkaline iron (III) reduction by a novel alkaliphilic, halotolerant, Bacillus sp. isolated from salt flat sediments of Soap Lake, Appl. Microbiol. Biotechnol. 77 (4) (2007) 927–934, https://doi.org/10.1007/s00253-007-1220-5.

[10] I.D. Sorokin, I.K. Kravchenko, E.V. Doroshenko, E.S. Boulygina, E.V. Zadorina, T.P. Tourova, D.Y. Sorokin, Haloalkaliphilic diazotrophs in soda solonchak soils, FEMS (Fed. Eur. Microbiol. Soc.) Microbiol. Ecol. 65 (3) (2008) 425–433, https://doi.org/10.1111/j.1574-6941.2008.00542.x.

[11] M. Delgado-García, S.M. Contreras-Ramos, J.A. Rodríguez, J.C. Mateos-Díaz, C.N. Aguilar, R.M. Camacho-Ruíz, Isolation of halophilic bacteria associated with saline and alkaline-sodic soils by culture dependent approach, Heliyon 4 (11) (2018) e00954, https://doi.org/10.1016/j.heliyon.2018.e00954.

[12] W. Xiao, Z.G. Wang, Y.X. Wang, M.A. Schneegurt, Z.Y. Li, Y.H. Lai, X.L. Cui, Comparative molecular analysis of the prokaryotic diversity of two salt mine soils in southwest China, J. Basic Microbiol. 53 (11) (2013) 942–952, https://doi.org/10.1002/jobm.201200200.

[13] S. Chen, Y. Xu, L. Helfant, Geographical isolation, buried depth, and physicochemical traits drive the variation of species diversity and prokaryotic community in three typical hypersaline environments, Microorganisms 8 (1) (2020) 120, https://doi.org/10.3390/microorganisms8010120.

[14] F. Wu, Y. Zhang, D. He, J. Gu, Q. Guo, X. Liu, H. Feng, Community structures of bacteria and archaea associated with the biodeterioration of sandstone sculptures at the Beishiku Temple, Int. Biodeterior. Biodegrad. 164 (2021) 105290, https://doi.org/10.1016/j.ibiod.2021.105290.

[15] A.V. Bryanskaya, A.A. Shipova, A.S. Rozanov, O.A. Kolpakova, E.V. Lazareva, Y.E. Uvarova, S.E. Peltek, Diversity and metabolism of microbial communities in a hypersaline lake along a geochemical gradient, Biology 11 (4) (2022) 605, https://doi.org/10.3390/biology11040605.

[16] A. Simachew, A. Lanzén, A. Gessesse, L. Øvreås, Prokaryotic community diversity along an increasing salt gradient in a soda ash concentration pond, Microb. Ecol. 71 (2) (2016) 326–338, https://doi.org/10.1007/s00248-015-0675-7.

[17] Z. Zhou, C. Wang, Y. Luo, Meta-analysis of the impacts of global change factors on soil microbial diversity and functionality, Nat. Commun. 11 (2020) 3072, https://doi.org/10.1038/s41467-020-16881-7.

[18] A. Kalwasińska, E. Deja-Sikora, A. Szabó, T. Felföldi, P. Kosobucki, M. Brzezinska, M. Walczak, Salino-alkaline lime of anthropogenic origin a reservoir of diverse microbial communities, Sci. Total Environ. 655 (2019) 842–854, https://doi.org/10.1016/j.scitotenv.2018.11.246.

[19] E.M. Brito, H.A. Piñón-Castillo, R. Guyoneaud, A. Caretta, J.F. Gutiérrez-Corona, R. Duran, M. Goñi-Urriza, Bacterial biodiversity from anthropogenic extreme environments: a hyper-alkaline and hyper-saline industrial residue contaminated by chromium and iron, Appl. Microbiol. Biotechnol. 97 (1) (2013) 369–378, https://doi.org/10.1007/s00253-012-3923-5.

[20] P.K. Dhal, P. Sar, Microbial communities in uranium mine tailings and mine water sediment from Jaduguda U mine, India: a culture independent analysis, Journal of Environmental Science and Health, Part A 49 (6) (2014) 694–709, https://doi.org/10.1080/10934529.2014.865458.

[21] L.A. Macías-Pérez, C. Levard, M. Barakat, B. Angeletti, D. Borschneck, L. Poizat, W. Achouak, M. Auffan, Contrasted microbial community colonization of a bauxite residue deposit marked by a complex geochemical context, J. Hazard Mater. 424 (2022) 127470, https://doi.org/10.1016/j.jhazmat.2021.127470. Part B.

[22] L. Jin, J.R. Gerson, J.D. Rocca, E.S. Bernhardt, M. Simonin, Alkaline mine drainage drives stream sediment microbial community structure and function, Sci. Total Environ. 805 (2022) 50189, https://doi.org/10.1016/j.scitotenv.2021.150189.

[23] W. Wang, Y. Yi, Y. Yang, Y. Zhou, S. Zhang, X. Wang, Z. Yang, Impact of anthropogenic activities on the sediment microbial communities of Baiyangdian shallow lake, Int. J. Sediment Res. 35 (2) (2020) 180–192, https://doi.org/10.1016/j.ijsrc.2019.10.006.

[24] N.F. Fetisova, V.V. Fetisov, M. De Maio, I.S. Zektser, Groundwater vulnerability assessment based on calculation of chloride travel time through the unsaturated zone on the area of the Upper Kama potassium salt deposit, Environ. Earth Sci. 75 (8) (2016) 681, https://doi.org/10.1007/s12665-016-5496-6.

[25] P.A. Belkin, Chemical composition of spring discharge in the area of mining waste storage and potassium salt enrichment, Bulletin of perm university. Geology 19 (3) (2020) 232–240, https://doi.org/10.17072/psu.geol.19.3.232 (In Russian).

[26] E. Khayrulina, A. Bogush, L. Novoselova, N. Mitrakova, Properties of alluvial soils of taiga forest under anthropogenic salinisation, Forests 12 (2021) 321, https://doi.org/10.3390/f12030321.

[27] E. Ushakova, A. Perevoshchikova, E. Menshikova, E. Khayrulina, R. Perevoshchikov, P. Belkin, Environmental aspects of potash mining: a case study of the Verkhnekamskoe potash deposit, Mining 3 (2023) 176–204, https://doi.org/10.3390/mining3020011.

[28] S. Krasilnikova, S. Blinov, P. Krasilnikov, P. Belkin, World experience using of soda production waste, Ecology and Industry of Russia 25 (12) (2021) 48–53, https://doi.org/10.18412/1816-0395-2021-12-48-53 (In Russian).

[29] S.S. Vaganov, R.D. Perevoshchikov, E.A. Menshikova, E.S. Ushakova, Method for sampling bottom sediments for environmental studies and a device for its implementation, RU Patent № 2762631 (2021).

[30] S.T. Bates, J.G. Berg-Lyons, W.A. Caporaso, W.A. Walters, R. Knight, N. Fierer, Examining the global distribution of dominant archaeal populations in soil, ISME J. 5 (2010) 908–917.

[31] S. Andrews, FastQC: A Quality Control Tool for High Throughput Sequence Data; Babraham Bioinformatics, Babraham Institute, Cambridge, UK, 2010.

[32] A.M. Bolger, M. Lohse, B. Usadel, Trimmomatic: a flexible trimmer for Illumina sequence data, Bioinformatics 30 (15) (2014) 2114–2120, https://doi.org/10.1093/bioinformatics/btu170.

[33] B.J. Callahan, P.J. McMurdie, M.J. Rosen, A.W. Han, A.J.A. Johnson, S.P. Holmes, DADA2: high-resolution sample inference from Illumina amplicon data, Nat. Methods 13 (2016) 581–583, https://doi.org/10.1038/nmeth.3869.

[34] E. Bolyen, J.R. Rideout, M.R. Dillon, et al., Reproducible, interactive, scalable and extensible microbiome data science using QIIME 2, Nat. Biotechnol. 37 (2019) 852–857, https://doi.org/10.1038/s41587-019-0209-9.

[35] Q. Wang, G. Garrity, J. Tiedje, J. Cole, Naïve Bayesian classifier for rapid assignment of rRNA sequences into the new bacterial taxonomy, Appl. Environ. Microbiol. 73 (2007) 5261–5267.

[36] C. Quast, E. Pruesse, P. Yilmaz, J. Gerken, T. Schweer, P. Yarza, F.O. Glöckner, The SILVA ribosomal RNA gene database project: improved data processing and web-based tools. Opens external link in new windowNucl, Nucleic Acids Res. 41 (D1) (2013) D590–D596.

[37] N.A. Bokulich, B.D. Kaehler, J.R. Rideout, M. Dillon, E. Bolyen, R. Knight, et al., Optimizing taxonomic classification of marker-gene amplicon sequences with qiime 2's q2-feature-classifier plugin, Microbiome 6 (2018) 90, https://doi.org/10.1186/s40168-018-0470-z.

[38] S. Lê, J. Josse, F. Husson, FactoMineR: an R package for multivariate analysis, J. Stat. Software 25 (2008) 1–18.

[39] P. McMurdie, S. Holmes, phyloseq: an R package for reproducible interactive analysis and graphics of microbiome census data, PLoS One 8 (2013) e61217.

[40] G.L. Simpson, ggvegan: 'ggplot2' plots for the 'vegan' package, R package version 0.1-0 (2019). Available online: https://www.rdocumentation.org/packages/ggvegan/versions/0.1-0. (Accessed 10 October 2022).

[41] F. Harrell, Package 'Hmisc': Harrell miscellaneous version 4.1-1. https://github.com/harrelfe/Hmisc, 2018.

[42] H. Wickham, ggplot2: Elegant Graphics for Data Analysis, Springer, 2016.

[43] H. Lin, S.D. Peddada, Analysis of compositions of microbiomes with bias correction, Nat. Commun. 11 (2020) 3514, https://doi.org/10.1038/s41467-020-17041-7.

[44] N.A. Grigoriev, Chemical Element Distribution in the Upper Continental Crust. Russia, Ekaterinburg: UrO RAN, 2009 (in Russian).

[45] A. Oren, Microbial life at high salt concentrations: phylogenetic and metabolic diversity, Saline Syst. 4 (1) (2008) 1–13.

[46] D. Paul, S.V. Kumbhare, S.S. Mhatre, S.P. Chowdhury, S.A. Shetty, N.P. Marathe, Y.S. Shouche, Exploration of microbial diversity and community structure of Lonar Lake: the only hypersaline meteorite crater lake within basalt rock, Front. Microbiol. 6 (2016) 1553.

[47] L.M. Cycil, S. DasSarma, W. Pecher, R. McDonald, M. AbdulSalam, F. Hasan, Metagenomic insights into the diversity of halophilic microorganisms indigenous to the Karak Salt Mine, Pakistan, Front. Microbiol. 11 (2020) 1567.

[48] Y. Wang, G. Bao, Diversity of prokaryotic microorganisms in alkaline saline soil of the Qarhan Salt Lake area in the Qinghai-Tibet Plateau, Sci. Rep. 12 (1) (2022) 3365, https://doi.org/10.1038/s41598-022-07311-3, 1.

[49] C.D. Vavourakis, R. Ghai, F. Rodriguez-Valera, D.Y. Sorokin, S.G. Tringe, P. Hugenholtz, G. Muyzer, Metagenomic insights into the uncultured diversity and physiology of microbes in four hypersaline soda lake brines, Front. Microbiol. 25 (7) (2016) 211, https://doi.org/10.3389/fmicb.2016.00211.

[50] J. Chakraborty, V. Sapkale, M. Shah, V. Rajput, G. Mehetre, S. Agawane, S. Dharne, Metagenome sequencing to unveil microbial community composition and prevalence of antibiotic and metal resistance genes in hypersaline and hyperalkaline Lonar Lake, India, Ecol. Indicat. 110 (2020) 105827, https://doi.org/10.1016/j.ecolind.2019.105827.

[51] E. Ersoy Omeroglu, M. Sudagidan, M.N.Z. Yurt, B.B. Tasbasi, E.E. Acar, V.C. Ozalp, Microbial community of soda Lake Van as obtained from direct and enriched water, sediment and fish samples, Sci. Rep. 11 (1) (2021) 1–13.

[52] E.B. Hollister, A.S. Engledow, A.J.M. Hammett, et al., Shifts in microbial community structure along an ecological gradient of hypersaline soils and sediments, ISME J. 4 (2010) 829–838, https://doi.org/10.1038/ismej.2010.3.

[53] M. Ben Abdallah, F. Karray, N. Kallel, et al., Abundance and diversity of prokaryotes in ephemeral hypersaline lake Chott El Jerid using Illumina Miseq sequencing, DGGE and qPCR assays, Extremophiles 22 (2018) 811–823, https://doi.org/10.1007/s00792-018-1040-9.

[54] R.A. Wilkes, L. Aristilde, Degradation and metabolism of synthetic plastics and associated products by Pseudomonas sp.: capabilities and challenges, J. Appl. Microbiol. 123 (3) (2017) 582–593.

[55] S.P. Biki, S. Mahmud, S. Akhter, M.J. Rahman, J.J. Rix, M.A. Al Bachchu, M. Ahmed, Polyethylene degradation by Ralstonia sp. strain SKM2 and Bacillus sp. strain SM1 isolated from land fill soil site, Environ. Technol. Innov. 22 (2021) 101495.

[56] M. Lin, X. Hu, W. Chen, H. Wang, C. Wang, Biodegradation of phenanthrene by Pseudomonas sp. BZ-3, isolated from crude oil contaminated soil, Int. Biodeterior. Biodegrad. 94 (2014) 176–181.

[57] S. Shariati, A.A. Pourbabaee, H.A. Alikhani, et al., Anaerobic biodegradation of phthalic acid by an indigenous Ralstonia pickettii strain SHAn2 isolated from Anzali international wetland, Int. J. Syst. Evol. Microbiol. 19 (2022) 4827–4838, https://doi.org/10.1007/s13762-021-03677-5.

[58] M. Youssef, E. Elshatoury, S. Ali, G. El-Taweel, Enhancement of phenol degradation by free and immobilized mixed culture of Providencia stuartii PL4 and Pseudomonas aeruginosa PDM isolated from activated sludge, Ann. Finance 23 (2019) 1–19, https://doi.org/10.1080/10889868.2019.1602106.

[59] W. Xu, Q. Zhao, Z. Li, X. Lu, S. Han, Z. Ye, Biodegradation of dinitrotoluene sulfonates and other nitro-aromatic compounds by Pseudomonas sp. X5 isolated from TNT red water contaminated soil, J. Clean. Prod. 214 (2019) 782–790, https://doi.org/10.1016/j.jclepro.2019.01.025.

[60] X. Huang, C.G. Weisener, J. Ni, B. He, D. Xie, Z. Li, Nitrate assimilation, dissimilatory nitrate reduction to ammonium, and denitrification coexist in Pseudomonas putida Y-9 under aerobic conditions, Bioresour. Technol. 312 (2020) 123597, https://doi.org/10.1016/j.biortech.2020.123597.

[61] Carpio I.E. Mejias, A. Ansari, D.F. Rodrigues, Relationship of biodiversity with heavy metal tolerance and sorption capacity: a meta-analysis approach, Environ. Sci. Technol. 52 (1) (2018) 184–194.

[62] R. Biswas, U. Halder, A. Kabiraj, A. Mondal, R. Bandopadhyay, Overview on the role of heavy metals tolerance on developing antibiotic resistance in both Gram-negative and Gram-positive bacteria, Arch. Microbiol. 203 (6) (2021) 2761–2770.

[63] P. Sharma, Efficiency of bacteria and bacterial assisted phytoremediation of heavy metals: an update, Bioresour. Technol. 328 (2021) 124835.

[64] C.A. Lozupone, R. Knight, Global patterns in bacterial diversity, Proc. Natl. Acad. Sci. USA 104 (27) (2007) 11436–11440.

[65] J.R. Osman, C. Regeard, C. Badel, G. Fernandes, M. DuBow, Variation of bacterial biodiversity from saline soils and estuary sediments present near the Mediterranean Sea coast of Camargue (France), Antonie Leeuwenhoek 112 (2019) 351–365, https://doi.org/10.1007/s10482-018-1164-z.

[66] A. Kalwasińska, T. Felföldi, A. Szabó, E. Deja-Sikora, P. Kosobucki, M. Walczak, Microbial communities associated with the anthropogenic, highly alkaline environment of a saline soda lime, Poland, Antonie Leeuwenhoek 110 (7) (2017) 945–962, https://doi.org/10.1007/s10482-017-0866-y.